(12)

NSWCDD/TR-93/351

TRACKING WITH TIME-DELAYED DATA IN MULTISENSOR SYSTEMS

BY RICHARD D. HILTON DAVID A. MARTIN WILLIAM D. BLAIR
SYSTEMS RESEARCH AND TECHNOLOGY DEPARTMENT

AUGUST 1993

NAVAL SURFACE WARFARE CENTER
DAHLGREN DIVISION
DAHLGREN, VIRGINIA 22448-5000

56793

NSWCDD/TR-93/351

TRACKING WITH TIME-DELAYED DATA IN MULTISENSOR SYSTEMS

BY RICHARD D. HILTON DAVID A. MARTIN WILLIAM D. BLAIR
SYSTEMS RESEARCH AND TECHNOLOGY DEPARTMENT

AUGUST 1993

NAVAL SURFACE WARFARE CENTER
DAHLGREN DIVISION
Dahlgren, Virginia 22448-5000

FOREWORD

The introduction of intership data networking into the process of target tracking by multiple platform sensors has raised the question of how to deal with remote sensor data that has arrived for fusion processing after a delay due to network loading. Conditions frequently arise wherein standard Kalman filtering formulations must be modified to be able to accept and meaningfully process late data. This report presents results of research into the relative efficacy of a complex, rationally derived modified Kalman filter update versus faster and simpler but *ad hoc* Kalman filter modifications for accepting late data. This work was conducted under the sponsorship of the Naval Surface Warfare Center Dahlgren Division (NSWCDD) AEGIS Program Office.

This document has been reviewed by Dr. T.R. Rice, Senior Physicist, Combat Systems Technology Group.

Approved by:

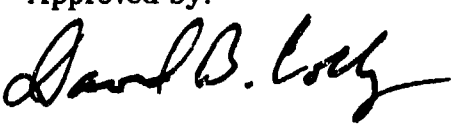

DAVID B. COLBY, Head
Systems Research and Technology

ABSTRACT

When techniques for target tracking are expanded to make use of multiple sensors in a multiplatform system, the possibility of time delayed data becomes a reality. When a discrete-time Kalman filter is applied and some of the data entering the filter are delayed, proper processing of these late data is a necessity for obtaining an "optimal" estimate of a target's state. If this problem is not given special care, the quality of the state estimates can be degraded relative to that quality provided by a single sensor. A negative-time update technique is developed using the criteria of minimum mean-square error (MMSE) under the constraint that only the results of the most recent update are saved. The performance of the MMSE technique is compared to that of the *ad hoc* approach employed in the Cooperative Engagement Capabilities (CEC) system for processing data from multiple platforms. It was discovered that the MMSE technique is a stable solution to the negative-time update problem, while the CEC technique was found to be less than desirable when used with filters designed for tracking highly maneuvering targets at relatively low data rates. The MMSE negative-time update technique was found to be a superior alternative to the existing CEC negative-time update technique.

CONTENTS

CHAPTER 1

INTRODUCTION

When techniques for target tracking are expanded to make use of multiple sensors in a multiplatform system, the possibility of time delayed data becomes a reality. When a discrete-time Kalman filter is applied and some of the data entering the filter are delayed, proper processing of these late data is a necessity for obtaining an "optimal" estimate of a target's state. If this problem, which may arise whenever data from dispersed sensors are fused, is not given special care, the quality of the state estimates can be degraded relative to that quality provided by a single sensor.

The optimal solution to this problem of processing late data requires the filter algorithm to return to the state estimate and error covariance that occurred just prior to the time corresponding to the late measurement. Then the filter process is restarted from the time of the late measurement. Thus, all the measurement information in the time interval between the most recent measurement and the late measurement must be saved to complete this filtering of past data. In order to bound the amount of information to be saved, a maximum for the delay time must be declared. Thus, all measurements, state estimates, and error covariances within the delay interval must be saved. This filtering approach that minimizes the mean-square error may not be practical in many cases. For example, when a tracking system is required to maintain current state estimates on many targets, storing the past information can become cumbersome.

In this report, the problem of updating the state estimate with late data is considered for the case where only the most recent state estimate and error covariance is saved. A solution is derived for this problem using a minimum mean-square error (MMSE) criteria. While the target state estimate provided by this approach will be inferior to that provided by the optimal MMSE approach that is described above, this suboptimal approach involves only modifying the state estimate produced with the most recent measurement using the late measurement.

Figure 1-1 illustrates a case wherein one of two sensors sends data to the site of fusion by way of a data network. In the illustrated network, the input queue is susceptible to being crowded by other traffic, causing measurements from sensor 2 to arrive at the site of data fusion late. Due to the late arrival, a filter update is made using measurements from only sensor 1, and if the measurement from sensor 2 is to be utilized, it will require special treatment. In this report, the process of using late measurements to improve the

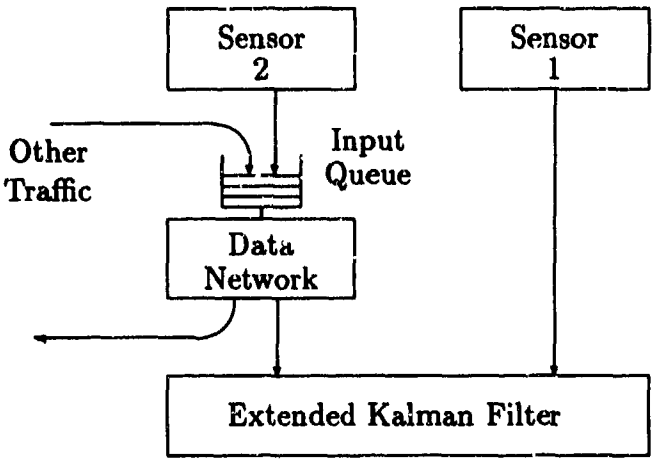

Figure 1–1. A Kalman Filter Receiving Delayed Measurements

current state estimate will be referred to as a negative-time update; and the time interval between the most recent measurement and the late measurement will be referred to as the negative-time interval. Some authors refer to the subject-matter as "data senescence."

The need for management of negative-time intervals arises in the tracking techniques used for implementation of Cooperative Engagement Capabilities (CEC). It was discovered in the Software Requirements Specification (SRS) document of CEC [1], that an *ad hoc* approach for handling negative-time measurements is used. A major motivation for undertaking this study was to examine the efficiency and robustness of the *ad hoc* treatment of delayed data within its environment – an *extended* Kalman filter of the sort described in Appendix A. An MMSE approach for handling negative-time updates is derived and used as a baseline for evaluating the specified CEC approach. The specified CEC updating method will be simulated as a separate program and will not be tested within a full simulation of the CEC system.

This report is organized in the following manner: Chapter 2 discusses the problem formulation and background information. Chapter 3 presents the development and derivation of the MMSE negative-time approach along with a simple numerical example of its implementation and an analysis of constant velocity tracking with a negative-time update. Chapter 4 discloses an interpretation of the CEC approach with a numerical example and analysis to parallel that in Chapter 3. Chapter 5 contains details and results of Monte Carlo simulations used to evaluate the performance of the *ad hoc* approach in a simplified but realistic context. Chapter 6 presents conclusions of the analysis.

CHAPTER 2

BACKGROUND AND PROBLEM FORMULATION

In this study, an extended Kalman filter is used to update a multiple source track file by processing measurements of range, bearing, and elevation. The study employs a simplified two-ship communications scenario in which an ownship sensor is tracking a maneuvering target while also receiving track contacts from a remote ship sensor tracking the same target. The two ships are confined to the (East-West) x-axis in order to eliminate the need for reference frame rotation; and the earth's shape is considered locally flat for simplicity.

Background

In CEC, every Cooperative Unit (CU) platform maintains target tracks in its own local coordinate system. Each CU uses its own sensors and broadcasts all of its sensor measurements in its own coordinate system. Periodically, each CU broadcasts information on its own position. When ownship receives a remote sensor measurement, it must take into account the coordinate system conversion when formulating the Kalman filter innovation term for tracking at ownship. The dynamics and measurement models assumed for the target in track are given by

$$X_{k+1} = F_k X_k + G_k w_k \tag{2.1}$$

$$Z_k = h_k(X_k) + v_k \tag{2.2}$$

where $w_k \sim N(0, Q_k)$ is the process error and $v_k \sim N(0, R_k)$ is the measurement error, respectively. Matrix F_k is the state transition matrix, G_k is the process error input matrix, and the target state X_k contains the position, velocity, and acceleration of the target. A linear measurement equation can be defined by linearizing the nonlinear observation function. The measurement equation, as a function of the actual target state, is given by

$$Z_k = \begin{bmatrix} r_k \\ b_k \\ e_k \end{bmatrix} = \begin{bmatrix} \sqrt{(x'_k)^2 + (y'_k)^2 + (z'_k)^2} \\ \tan^{-1}\left(\frac{y'_k}{x'_k}\right) \\ \tan^{-1}\left(\frac{z'_k}{\sqrt{(x'_k)^2 + (y'_k)^2}}\right) \end{bmatrix} + \begin{bmatrix} v_k^r \\ v_k^b \\ v_k^e \end{bmatrix} \tag{2.3}$$

where

$$x'_k = x_k - x_{ob} \tag{2.4}$$
$$y'_k = y_k - y_{ob} \tag{2.5}$$
$$z'_k = z_k - z_{ob} \tag{2.6}$$

and (x_k, y_k, z_k) correspond to the (x, y, z) coordinates of the target in the ownship reference frame at time k, and (x_{ob}, y_{ob}, z_{ob}) correspond to the origin of the remote ship in terms of the ownship reference frame at time k. Since we are neglecting motion between the two ships, x_{ob}, y_{ob}, and z_{ob} are constants. For ownship measurements, $(x_{ob}, y_{ob}, z_{ob}) = (0, 0, 0)$. The r_k, b_k, and e_k are the measured range, bearing, and elevation relative to the remote sensor reference frame at time k. The v_k^r, v_k^b, and v_k^e are the measurement errors for the range, bearing, and elevation at time k, respectively.

For a filter processing range, bearing, and elevation measurements,

$$h_k(X_k) = \begin{bmatrix} \sqrt{(x'_k)^2 + (y'_k)^2 + (z'_k)^2} \\ \tan^{-1}\left(\frac{y'_k}{x'_k}\right) \\ \tan^{-1}\left(\frac{z'_k}{\sqrt{(x'_k)^2 + (y'_k)^2}}\right) \end{bmatrix} \tag{2.7}$$

Using a first-order Taylor series to linearize (2.7) about the predicted state estimate results in the linearized measurement matrix given by

$$H_k = \begin{bmatrix} \frac{x'_{k|k-1}}{R_{k|k-1}} & 0 & \frac{y'_{k|k-1}}{R_{k|k-1}} & 0 & \frac{z'_{k|k-1}}{R_{k|k-1}} & 0 \\ \frac{-y'_{k|k-1}}{Rh_{k|k-1}} & 0 & \frac{x'_{k|k-1}}{Rh_{k|k-1}} & 0 & 0 & 0 \\ \frac{-z'_{k|k-1}x'_{k|k-1}}{Rh_{k|k-1}R^2_{k|k-1}} & 0 & \frac{-z'_{k|k-1}y'_{k|k-1}}{Rh_{k|k-1}R^2_{k|k-1}} & 0 & \frac{Rh_{k|k-1}}{R^2_{k|k-1}} & 0 \end{bmatrix} \tag{2.8}$$

where

$$X_k = [\ x_k \quad \dot{x}_k \quad y_k \quad \dot{y}_k \quad z_k \quad \dot{z}_k\ ]^T \tag{2.9}$$

$$R_{k|k-1} = \sqrt{(x'_{k|k-1})^2 + (y'_{k|k-1})^2 + (z'_{k|k-1})^2} \tag{2.10}$$

$$Rh_{k|k-1} = \sqrt{(x'_{k|k-1})^2 + (y'_{k|k-1})^2} \tag{2.11}$$

The equations for the extended Kalman filter are given as follows.

Time Update:

$$X_{k|k-1} = F_{k-1}X_{k-1|k-1} \tag{2.12}$$

$$P_{k|k-1} = F_{k-1}P_{k-1|k-1}F^T_{k-1} + G_{k-1}Q_{k-1}G^T_{k-1} \tag{2.13}$$

Measurement Update:

$$X_{k|k} = X_{k|k-1} + K_k[Z_k - h_k(X_{k|k-1})] \tag{2.14}$$

$$P_{k|k} = [I - K_kH_k]P_{k|k-1} \tag{2.15}$$

$$K_k = P_{k|k-1}H^T_k[H_kP_{k|k-1}H^T_k + R_k]^{-1} \tag{2.16}$$

The subscript notation $(k|j)$ refers to the estimate at time k given measurements through time j. The $P_{k|k}$ is the error covariance associated with the state estimate $X_{k|k}$, and K_k is the Kalman gain.

Problem Formulation

In Figure 2–1, a time line is given for a situation in which a negative-time update of a discrete time extended Kalman filter is necessary. At t_{k-2}, a normal filter update using timely data Z_{k-2}, results in state estimate $X_{k-2|k-2}$. At t_{k-1}, a remote sensor obtains a measurement Z_{k-1}; appends these data with the relevant time tag t_{k-1}; and submits a data message to a data network where its transmission is delayed. At t_k, another measurement

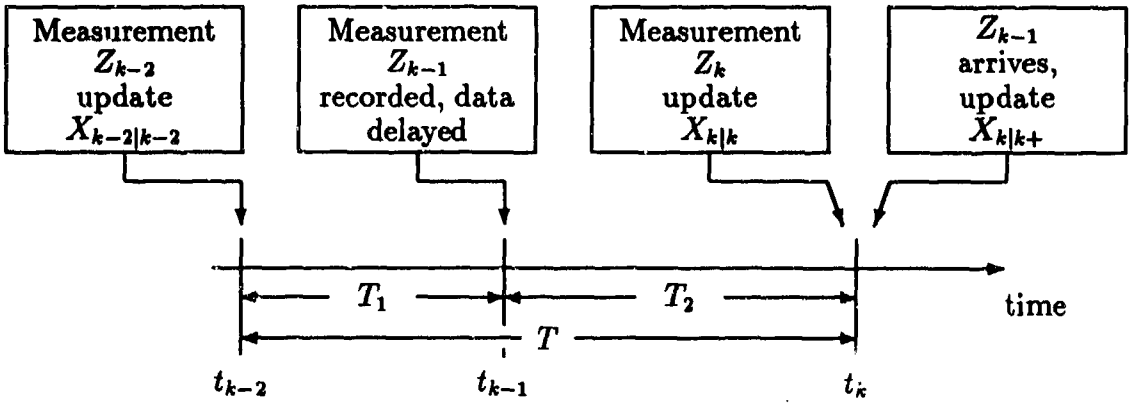

Figure 2–1. Time Line for Events Requiring a Negative-Time Update

Z_k from the ownship sensor arrives on time and is used to update the state estimate from $X_{k-2|k-2}$ to $X_{k|k}$. After this update takes place, at t_k^+, measurement Z_{k-1} with time tag t_{k-1} arrives after its delayed transmission. An approach to incorporate this delayed data into an "improved" state estimate $X_{k|k+}$ is developed in the next chapter. A related problem has been studied by Thomopoulos and Zhang [2], wherein data reaches a fusion site after a delay whose duration is known statistically but not exactly (that is, when no time tag t_{k-1} is appended to the measurement). Their formulations bear some resemblance to the results obtained in the next chapter.

CHAPTER 3

MINIMUM MEAN-SQUARE ERROR APPROACH

This chapter undertakes the derivation of a negative-time update algorithm built upon the problem formulation of the previous chapter. This approach will be referred to as a minimum mean-square error (MMSE) approach. This chapter also includes a simple example to display the use of this approach, and compares its performance with other methods of incorporating time-delayed data.

State Evolution

Referring to Figure 2–1, the illustrated intervals of time will be denoted as

$$T \triangleq t_k - t_{k-2} \tag{3.1}$$

$$T_1 \triangleq t_{k-1} - t_{k-2} \tag{3.2}$$

$$T_2 \triangleq t_k - t_{k-1} \tag{3.3}$$

The error in a state estimate $X_{k|j}$ will be denoted by $\widetilde{X}_{k|j}$ and is related to true state X_k by

$$X_k = X_{k|j} + \widetilde{X}_{k|j} \tag{3.4}$$

The discrete-time evolution of state $X_{k|k} \in \mathcal{R}^n$ over the time interval T is represented as

$$X_k = F(T)X_{k-2} + W(T) \tag{3.5}$$

where F is the discrete time state transition matrix and $W(T)$ is a vector representing the effects of plant noise that accrued during T. Throughout the remainder of this discussion, it will be assumed that state vector $X_k = [\ x_k \quad \dot{x}_k\ ]^T$ is one (uncoupled) dimension in a two- or three-dimensional constant velocity filter. The state transition matrix then is

$$F(T) = \begin{bmatrix} 1 & T \\ 0 & 1 \end{bmatrix} \tag{3.6}$$

The plant noise for this model will be a continuous-time, white noise acceleration. A unit impulse acceleration $\delta(t - \alpha)$, with $t_{k-2} < \alpha < t_k$, will bring about the response in state space of $[\ (t_k - \alpha) \quad 1\ ]^T$. A white noise acceleration $w(\alpha)$ where

$$E\{w(\alpha)\} = 0, \quad E\{w(\alpha)w(\beta)\} = \overline{q} \cdot \delta(\alpha - \beta) \tag{3.7}$$

applied throughout the time interval T brings about (by superposition) the plant noise

$$W(T) = \int_{t_{k-2}}^{t_k} \begin{bmatrix} t_k - \alpha \\ 1 \end{bmatrix} w(\alpha) d\alpha \tag{3.8}$$

The time projection of state estimate covariance from t_{k-2} to t_k is

$$P_{k|k-2} = F(T) P_{k-2|k-2} F^T(T) + E \left\{ \int_{t_{k-2}}^{t_k} \begin{bmatrix} t_k - \alpha \\ 1 \end{bmatrix} w(\alpha) d\alpha \int_{t_{k-2}}^{t_k} \begin{bmatrix} t_k - \beta \\ 1 \end{bmatrix}^T w(\beta) d\beta \right\} \tag{3.9}$$

or

$$P_{k|k-2} = F(T) P_{k-2|k-2} F^T(T) + Q(T) \tag{3.10}$$

with

$$Q(T) = \begin{bmatrix} \frac{1}{3}T^3 & \frac{1}{2}T^2 \\ \frac{1}{2}T^2 & T \end{bmatrix} \overline{q} \tag{3.11}$$

where $\overline{q}$ is a scalar parameter in units of $(length^2)/(time^3)$. This scalar quantifies the uncertainty in the (constant velocity) model of target dynamics and will be referred to as the "variance of acceleration error." Thus, when the time interval T is broken into two segments, T_1 and T_2, the state transitions are

$$X_{k-1} = F(T_1) X_{k-2} + \int_{t_{k-2}}^{t_{k-1}} \begin{bmatrix} t_{k-1} - \alpha \\ 1 \end{bmatrix} w(\alpha) d\alpha \tag{3.12}$$

$$X_k = F(T_2) X_{k-1} + \int_{t_{k-1}}^{t_k} \begin{bmatrix} t_k - \alpha \\ 1 \end{bmatrix} w(\alpha) d\alpha \tag{3.13}$$

and the projected covariance for the segmented time interval is given by

$$P_{k-1|k-2} = F(T_1) P_{k-2|k-2} F^T(T_1) + Q(T_1) \tag{3.14}$$

$$P_{k|k-1} = F(T_2) P_{k-1|k-1} F^T(T_2) + Q(T_2) \tag{3.15}$$

where

$$Q(T_1) = \begin{bmatrix} \frac{1}{3}T_1^3 & \frac{1}{2}T_1^2 \\ \frac{1}{2}T_1^2 & T_1 \end{bmatrix} \overline{q} \tag{3.16}$$

$$Q(T_2) = \begin{bmatrix} \frac{1}{3}T_2^3 & \frac{1}{2}T_2^2 \\ \frac{1}{2}T_2^2 & T_2 \end{bmatrix} \overline{q} \tag{3.17}$$

Filter Update At t_k With Z_k

When the measurement Z_k arrives at the filter for processing, the filter does not know of the existence of the delayed measurement Z_{k-1}. Therefore, the filter will proceed with a

standard Kalman filter update processing using $T = t_k - t_{k-2}$, since t_{k-2} was the time tag on the last measurement that it received. The first stage of processing will project the previous state estimate $X_{k-2|k-2}$, which is comprised of the actual state less the estimation error

$$X_{k-2|k-2} = X_{k-2} - \widetilde{X}_{k-2|k-2} \tag{3.18}$$

using the standard time projection formula

$$X_{k|k-2} = F(T)X_{k-2|k-2} \tag{3.19}$$

Equation (3.5) shows that the error in the projected state estimate is

$$\widetilde{X}_{k|k-2} = F(T)\widetilde{X}_{k-2|k-2} + \int_{t_{k-2}}^{t_k} \begin{bmatrix} t_k - \alpha \\ 1 \end{bmatrix} w(\alpha)d\alpha \tag{3.20}$$

Standard extended Kalman filter processing then updates the state estimate using gain K_k and

$$X_{k|k} = X_{k|k-2} + K_k(Z_k - H_k X_{k|k-2}) \tag{3.21}$$

Using (3.20) in (3.21) and isolating X_k to $\widetilde{X}_{k|k}$ shows that

$$\begin{aligned} \widetilde{X}_{k|k} &= (I - K_k H_k)F(T)\widetilde{X}_{k-2|k-2} - K_k v_k \\ &\quad +(I - K_k H_k)\int_{t_{k-2}}^{t_{k-1}} \begin{bmatrix} t_k - \alpha \\ 1 \end{bmatrix} w(\alpha)d\alpha \qquad (3.22) \\ &\quad +(I - K_k H_k)\int_{t_{k-1}}^{t_k} \begin{bmatrix} t_k - \alpha \\ 1 \end{bmatrix} w(\alpha)d\alpha \qquad (3.23) \end{aligned}$$

To allow for the contingency that a negative-time update may be necessary at the time of update $X_{k-2|k-2} \rightarrow X_{k|k}$, it will be convenient to define the quantity

$$S_k \triangleq E\{\widetilde{X}_{k|k}\int_{t_{k-1}}^{t_k} \begin{bmatrix} t_k - \beta \\ 1 \end{bmatrix}^T w(\beta)d\beta\} \tag{3.24}$$

This quantity is the covariance between the state estimation error $\widetilde{X}_{k|k}$ after the standard update at t_k and the plant noise error that accumulated over a portion (T_2) of the previous time interval T. This covariance is now identifiable by substituting (3.23) into (3.24). The covariance is given by

$$\begin{aligned} S_k &= E\left\{(I - K_k H_k)F(T)\widetilde{X}_{k-2|k-2}\int_{t_{k-1}}^{t_k} \begin{bmatrix} t_k - \beta \\ 1 \end{bmatrix}^T w(\beta)d\beta \right. \\ &\quad +(I - K_k H_k)\int_{t_{k-2}}^{t_{k-1}} \begin{bmatrix} t_k - \alpha \\ 1 \end{bmatrix} w(\alpha)d\alpha \int_{t_{k-1}}^{t_k} \begin{bmatrix} t_k - \beta \\ 1 \end{bmatrix}^T w(\beta)d\beta \\ &\quad +(I - K_k H_k)\int_{t_{k-1}}^{t_k} \begin{bmatrix} t_k - \alpha \\ 1 \end{bmatrix} w(\alpha)d\alpha \int_{t_{k-1}}^{t_k} \begin{bmatrix} t_k - \beta \\ 1 \end{bmatrix}^T w(\beta)d\beta \\ &\quad \left. -K_k v_k \int_{t_{k-1}}^{t_k} \begin{bmatrix} t_k - \beta \\ 1 \end{bmatrix}^T w(\beta)d\beta \right\} \end{aligned} \tag{3.25}$$

Distributing the expected value through (3.25) gives

$$\begin{aligned} S_k &= (I - K_k H_k)F(T)E\left\{\widetilde{X}_{k-2|k-2}\int_{t_{k-1}}^{t_k}\begin{bmatrix} t_k-\beta \\ 1 \end{bmatrix}^T w(\beta)d\beta\right\} \\ &+(I-K_kH_k)E\left\{\int_{t_{k-2}}^{t_{k-1}}\begin{bmatrix} t_k-\alpha \\ 1 \end{bmatrix} w(\alpha)d\alpha\int_{t_{k-1}}^{t_k}\begin{bmatrix} t_k-\beta \\ 1 \end{bmatrix}^T w(\beta)d\beta\right\} \\ &+(I-K_kH_k)E\left\{\int_{t_{k-1}}^{t_k}\begin{bmatrix} t_k-\alpha \\ 1 \end{bmatrix} w(\alpha)d\alpha\int_{t_{k-1}}^{t_k}\begin{bmatrix} t_k-\beta \\ 1 \end{bmatrix}^T w(\beta)d\beta\right\} \\ &-K_kv_kE\left\{\int_{t_{k-1}}^{t_k}\begin{bmatrix} t_k-\beta \\ 1 \end{bmatrix}^T w(\beta)d\beta\right\} \end{aligned} \tag{3.26}$$

Eliminating expectations of uncorrelated random processes and evaluating the single remaining term yields

$$S_k = (I - K_k H_k)Q(T_2) \tag{3.27}$$

which is the sought-after covariance that will appear in subsequent formulations.

Negative-Time Update Algorithm

When the occurrence of a delayed measurement Z_{k-1} having error $v_{k-1} \sim N(0, R_{k-1})$ comes to light *after* the state estimate update $X_{k|k}$, a second state estimate update $X_{k|k+}$ using an as-yet undetermined Kalman gain K_{k+} at t_k^+ will be made. The form to be used is

$$X_{k|k+} = X_{k|k} + K_{k+}[Z_{k-1} - H_{k-1}F^{-1}(T_2)X_{k|k}] \tag{3.28}$$

Note that the term $F^{-1}(T_2)X_{k|k}$ is used to compute the innovation of the update at time t_{k-1} while keeping the time of the estimate $X_{k|k+}$ at t_k. Using $Z_{k-1} = H_{k-1}X_{k-1} + v_{k-1}$ and using (3.13) in (3.28) yields

$$\widetilde{X}_{k|k+} = [I - K_{k+}H_{k-1}F^{-1}(T_2)]\widetilde{X}_{k|k} + K_{k+}H_{k-1}F^{-1}(T_2)\int_{t_{k-1}}^{t_k}\begin{bmatrix} t_k-\alpha \\ 1 \end{bmatrix} w(\alpha)d\alpha - K_{k+}v_{k-1} \tag{3.29}$$

The modified Kalman gain K_{k+} is now found by

1. Using (3.29) to express $P_{k|k+} = E\{\widetilde{X}_{k|k+}\widetilde{X}_{k|k+}^T\}$
2. Setting $\dfrac{\partial}{\partial K_{k+}} trace(P_{k|k+})$ to zero
3. Solving for K_{k+}

In so doing, it is useful to note that [4]

$$\frac{\partial}{\partial A} trace(BAC) = B^T C^T \tag{3.30}$$

$$\frac{\partial}{\partial A} trace(ABA^T) = A(B + B^T) \tag{3.31}$$

The covariance $P_{k|k+} = E\{\widetilde{X}_{k|k+}\widetilde{X}^T_{k|k+}\}$ is found from (3.29) to be

$$\begin{aligned} P_{k|k+} = & [I - K_{k+}H_{k-1}F^{-1}(T_2)]P_{k|k}[I - K_{k+}H_{k-1}F^{-1}(T_2)]^T \\ & + [I - K_{k+}H_{k-1}F^{-1}(T_2)]S_k F^{-T}(T_2)H^T_{k-1}K^T_{k+} \\ & + K_{k+}H_{k-1}F^{-1}(T_2)S^T_k[I - K_{k+}H_{k-1}F^{-1}(T_2)]^T \\ & + K_{k+}[H_{k-1}F^{-1}(T_2)Q(T_2)F^{-T}(T_2)H^T_{k-1} + R_{k-1}]K^T_{k+} \end{aligned} \tag{3.32}$$

where $F^{-T} = (F^{-1})^T$. Setting the derivative of the trace to zero gives

$$\begin{aligned} \frac{\partial}{\partial K_{k+}} trace(P_{k|k+}) = & -2P_{k|k}F^{-T}(T_2)H^T_{k-1} \\ & + 2K_{k+}[H_{k-1}F^{-1}(T_2)\{P_{k|k} - S_k - S^T_k + Q(T_2)\}F^{-T}(T_2)H^T_{k-1} \\ & + R_{k-1}] + 2S_k F^{-T}(T_2)H^T_{k-1} = 0 \end{aligned} \tag{3.33}$$

Solving for the modified Kalman gain for a late measurement K_{k+} yields

$$\begin{aligned} K_{k+} = & (P_{k|k} - S_k)F^{-T}(T_2)H^T_{k-1} \times \\ & [H_{k-1}F^{-1}(T_2)\{P_{k|k} - S_k - S^T_k + Q(T_2)\}F^{-T}(T_2)H^T_{k-1} + R_{k-1}]^{-1} \end{aligned} \tag{3.34}$$

Manipulating (3.32) into the form

$$\begin{aligned} P_{k|k+} = & K_{k+}[H_{k-1}F^{-1}(T_2)\{P_{k|k} - S_k - S^T_k + Q(T_2)\}F^{-T}H^T_{k-1} + R_{k-1}]K^T_{k+} \\ & + P_{k|k} - K_{k+}H_{k-1}F^{-1}(T_2)[P_{k|k} - S^T_k] \\ & - [P_{k|k} - S_k]F^{-T}(T_2)H^T_{k-1}K^T_{k+} \end{aligned} \tag{3.35}$$

and substituting (3.34) into the first K_{k+} term of (3.35) gives

$$P_{k|k+} = [I - K_{k+}H_{k-1}F^{-1}(T_2)]P_{k|k} + K_{k+}H_{k-1}F^{-1}(T_2)S^T_k \tag{3.36}$$

which together with (3.34) and (3.28) completes the negative-time update. This negative-time update algorithm will be referred to as the MMSE approach.

Simple Numerical Example

To compare the MMSE negative-time approach with the standard Kalman filter formulation, when no negative times are encountered, a simple numerical example is presented

that uses the Kalman filter for one coordinate of a target track. The filter parameters are

$$X_k = \begin{bmatrix} x_k \\ \dot{x}_k \end{bmatrix} \tag{3.37}$$

$$F_k(T) = \begin{bmatrix} 1 & T \\ 0 & 1 \end{bmatrix} \tag{3.38}$$

$$H_k = \begin{bmatrix} 1 & 0 \end{bmatrix} \tag{3.39}$$

$$R_k = 144.0 \tag{3.40}$$

$$\bar{q} = 5.0 \tag{3.41}$$

where the plant noise is computed using (3.11). A useful parameter for characterizing this tracking filter is the tracking index μ_c in [3] given by

$$\mu_c = \sqrt{T^3 \frac{\bar{q}}{R_k}} = 0.186 \tag{3.42}$$

The tracking index is often useful for characterizing tracking filters since it defines an α, β filter having gains equivalent to the steady-state Kalman gains. For this example the initial covariance was set at

$$P_{0|0} = \begin{bmatrix} 79 & 32 \\ 32 & 26 \end{bmatrix} \tag{3.43}$$

A baseline case is now tabulated with four measurements, Z_k, $k = 1, 2, 3, 4$, all arriving on time at 1 sec intervals. Only the error covariance updates are tabulated. The equations used are the standard Kalman filter equations given by

$$P_{k|k-1} = F(T) P_{k-1|k-1} F^T(T) + Q_{k-1}(T) \tag{3.44}$$

$$K_k = P_{k|k-1} H_k^T [H_k P_{k|k-1} H_k^T + R_k]^{-1} \tag{3.45}$$

$$P_{k|k} = (I - K H_k) P_{k|k-1} \tag{3.46}$$

The results are presented in Table 3–1. Table 3–2 shows the evolution of the error covariance matrix for the case of measurement Z_3 missing altogether. The final measurement Z_4 retains the subscript 4 to conform to the indexing conventions used in the previous section. Note that the time interval T increases to 2 sec and that the elements in $P_{4|2}$ are quite large. The Kalman gain K_4 is also high, causing the trace of $P_{4|4}$ to increase significantly over that of the baseline case.

The negative-time update formulations are now to be employed. It is supposed that after the update, resulting in $P_{4|4}$ with Z_3 missing, has taken place (but before any subsequent updates), Z_3 arrives late. First, the covariance S_k is found by (3.27) to be

$$S_4 = (I - K_4 H_4) Q(1) = \begin{bmatrix} 0.6100 & 0.9000 \\ 2.2000 & 4.5000 \end{bmatrix} \tag{3.47}$$

Using $P_{4|4}$ and S_4 in (3.34) yields

$$K_{4+} = \begin{bmatrix} 0.3375 \\ 0.0591 \end{bmatrix} \tag{3.48}$$

Table 3–1. Baseline Result With All Measurements On Time

k	T	$P_{k\|k-1}$	K_k	$P_{k\|k}$
1	1	$\begin{bmatrix} 163.67 & 60.50 \\ 60.50 & 31.00 \end{bmatrix}$	$\begin{bmatrix} 0.5320 \\ 0.1966 \end{bmatrix}$	$\begin{bmatrix} 76.60 & 28.32 \\ 28.32 & 19.10 \end{bmatrix}$
2	1	$\begin{bmatrix} 154.00 & 49.92 \\ 49.92 & 24.10 \end{bmatrix}$	$\begin{bmatrix} 0.5168 \\ 0.1675 \end{bmatrix}$	$\begin{bmatrix} 74.42 & 24.12 \\ 24.12 & 15.74 \end{bmatrix}$
3	1	$\begin{bmatrix} 140.07 & 42.36 \\ 42.36 & 20.74 \end{bmatrix}$	$\begin{bmatrix} 0.4931 \\ 0.1491 \end{bmatrix}$	$\begin{bmatrix} 71.00 & 21.47 \\ 21.47 & 14.42 \end{bmatrix}$
4	1	$\begin{bmatrix} 130.04 & 38.40 \\ 38.40 & 19.42 \end{bmatrix}$	$\begin{bmatrix} 0.4745 \\ 0.1401 \end{bmatrix}$	$\begin{bmatrix} 68.33 & 20.18 \\ 20.18 & 14.04 \end{bmatrix}$

Table 3–2. Filter Result With Measurement Z_3 Discarded Altogether

k	T	$P_{k\|k-1}$	K_k	$P_{k\|k}$
1	1	$\begin{bmatrix} 163.67 & 60.50 \\ 60.50 & 31.00 \end{bmatrix}$	$\begin{bmatrix} 0.5320 \\ 0.1966 \end{bmatrix}$	$\begin{bmatrix} 76.60 & 28.32 \\ 28.32 & 19.10 \end{bmatrix}$
2	1	$\begin{bmatrix} 154.00 & 49.92 \\ 49.92 & 24.10 \end{bmatrix}$	$\begin{bmatrix} 0.5168 \\ 0.1675 \end{bmatrix}$	$\begin{bmatrix} 74.42 & 24.12 \\ 24.12 & 15.74 \end{bmatrix}$
3	–	—	—	—
4	2	$\begin{bmatrix} 247.20 & 65.60 \\ 65.60 & 25.74 \end{bmatrix}$	$\begin{bmatrix} 0.6319 \\ 0.1677 \end{bmatrix}$	$\begin{bmatrix} 91.00 & 24.15 \\ 24.15 & 14.74 \end{bmatrix}$

Table 3-3. Traces of Covariances $P_{4|4}$

CASE	TRACE
All measurements on time	82.376
Measurement Z_3 missing	105.734
Z_3 processed negative-time	82.376

and using this result in (3.36) yields

$$P_{4|4+} = \begin{bmatrix} 68.33 & 20.18 \\ 20.18 & 14.04 \end{bmatrix} \tag{3.49}$$

Table 3-3 compares the traces of these three final $P_{4|4}$ matrices. The performance of the MMSE approach results in a nearly full recovery of the filter covariance achieved when the measurement Z_3 arrived on time.

Negative-Time Updates and Constant Velocity Tracking

To compare the MMSE negative-time update with other methods for processing measurements with a negative-time increment, a scenario is considered in which there are two ships transmitting constant velocity track information periodically, and one measurement arrives after a delay that exceeds the sample period, as it does in the example of the previous section. This situation results in an out-of-sequence measurement for which a negative-time update technique must be utilized. A program was written to evaluate the effects on filter covariance of this single negative-time update when tracking a constant velocity target with various negative-time update formulations. Each evaluation includes a computation of filter covariance similiar to the numerical example of the previous section.

To assess the performance of negative-time update techniques for various tracking situations, the standard deviation of the measurement errors will be fixed at 25 m, while the standard deviation of the acceleration errors for the filter will be varied from 2 to 25 $m/s^{\frac{1}{2}}$. Sample periods of 0.25, 0.5, 1.0, and 2.0 sec will be considered. For this study, each of two sensors provides data at a sample interval of 2T, with the data from one sensor skewed by T relative to the other sensor. Thus, the measurements of the target's position are recorded periodically with period T and the filter will achieve steady-state conditions. The filter is assumed to be in steady-state conditions when a measurement from the remote sensor is delayed by more than T, and a negative-time update is needed. The starting covariance matrix for each computation is derived from the prevailing tracking index μ_c for each case. For the constant velocity tracking filter defined by (3.11) and (3.37)-(3.39), the steady-state

error covariance is given in [3] as

$$P_{SS} = P_{k-1|k-1} = R_k \begin{bmatrix} \alpha & \frac{\beta}{T} \\ \frac{\beta}{T} & \frac{\beta(2\alpha-\beta)}{2(1-\alpha)T^2} \end{bmatrix} \tag{3.50}$$

where

$$\beta = 6 - 3\alpha - \sqrt{3\alpha^2 - 36\alpha + 36} \tag{3.51}$$

$$\mu_c^2 = \frac{\beta^2}{1-\alpha} = \frac{T^3\bar{q}}{R_k} \tag{3.52}$$

With P_{SS} of (3.50) as the starting point, the usual Kalman filter equations were used to update the covariance matrix using a sample period of 2T to represent a skipped measurement. After the filter update with sample period of 2T is completed, the delayed measurement arrives and this information can be used to correct the state estimate and associated error covariance. Five techniques for processing the delayed measurement are considered. The first three are those illustrated in the previous section with the simple numerical example. The first technique (no late measurements) is an ideal case in which the measurement is not delayed at all. The second technique (discard late measurements) is put forth as a worst case – the results one obtains from not trying to cope with delayed data at all. The third technique (MMSE) is offered as a practical best case – the results one obtains when the trouble is taken to fully implement an optimized negative-time update formulation. The next two techniques illustrate the benefits and limitations of *ad hoc* techniques for negative-time updates. The fourth technique includes plant noise Q_k during the time update to the late measurement and during the time update back to the current time. The fifth technique sets the plant noise Q_k to zero during the time update to the late measurement and during the time update back to the current time.

The five techniques are compared using a plot of the normalized trace of the error covariance given by

$$P = \left\{ \frac{trace(P_{k|k+})}{R_k} \right\} \tag{3.53}$$

versus the standard deviation of the acceleration error. The results are given for each time period in Figures 3–1 through 3–4. Using all late measurements discarded as a worst case senario, it is seen that the technique using the plant noise throughout the negative update breaks down for relatively low levels of acceleration error. Breakdown of a negative-time update algorithm will be used to denote the condition at which the error covariance at time t_k is increased by processing a time-delayed measurement at time $t_k - \Delta$. However, the technique that has the plant noise set to zero during the negative update seems to be sufficient for shorter time periods, but becomes unrealistic for longer time periods in that the trace of the error covariance is lower than the optimal case where all measurements arrive sequentially (no late measurements). It is also noticed that the performance of the MMSE negative update closely matches that of the sequential case.

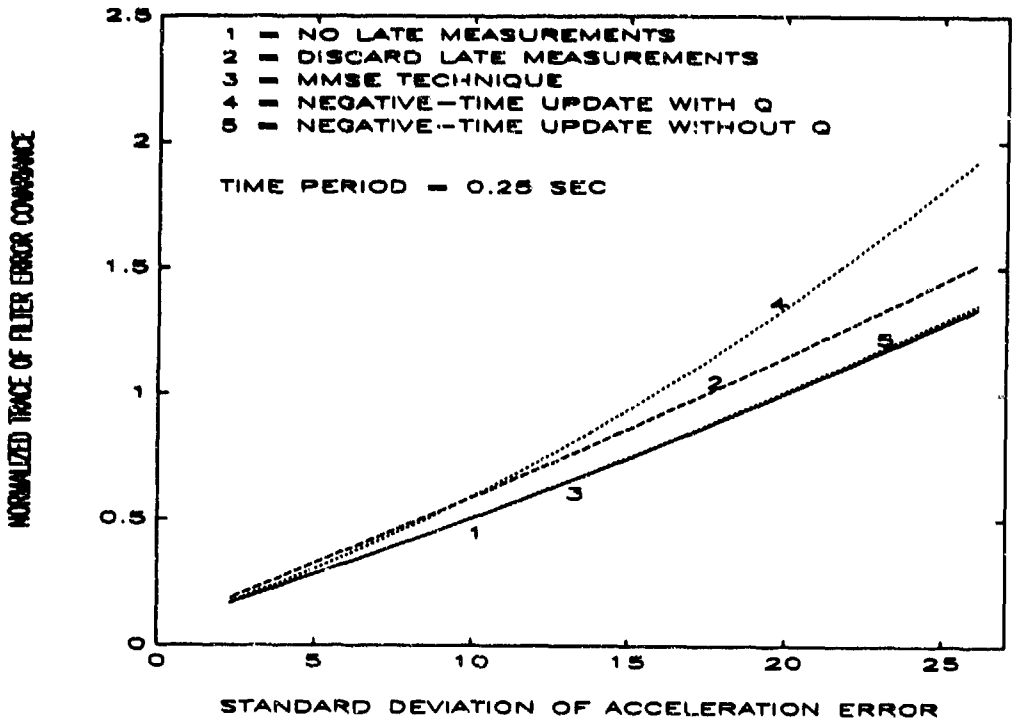

Figure 3–1. Negative-Time Update Technique Performance

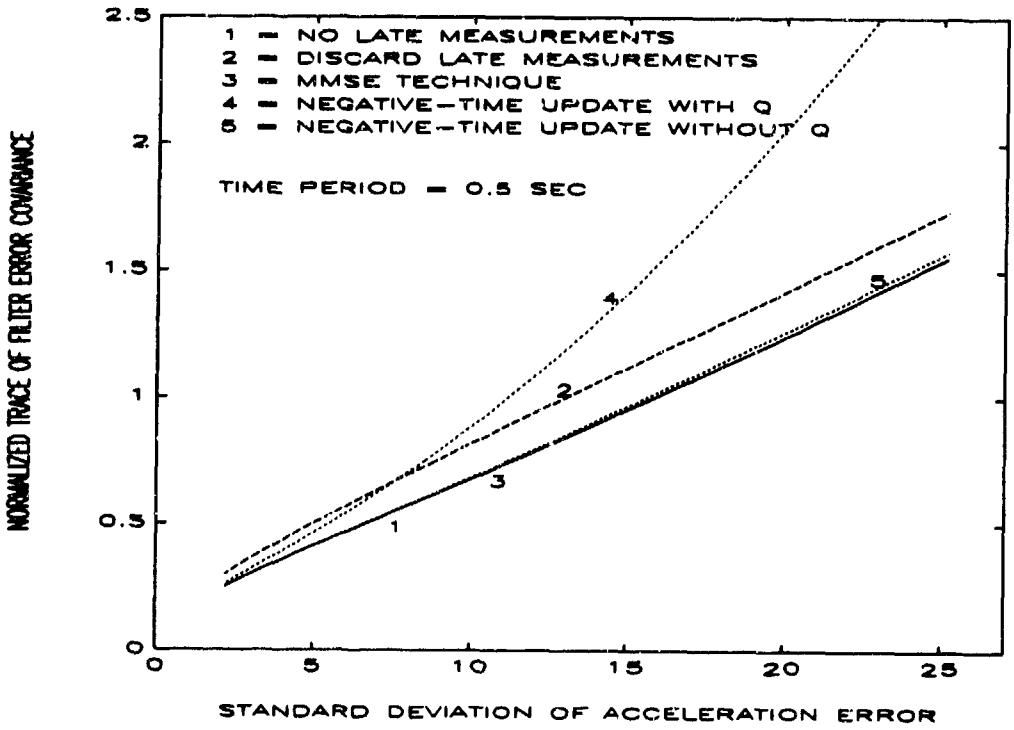

Figure 3–2. Negative-Time Update Technique Performance

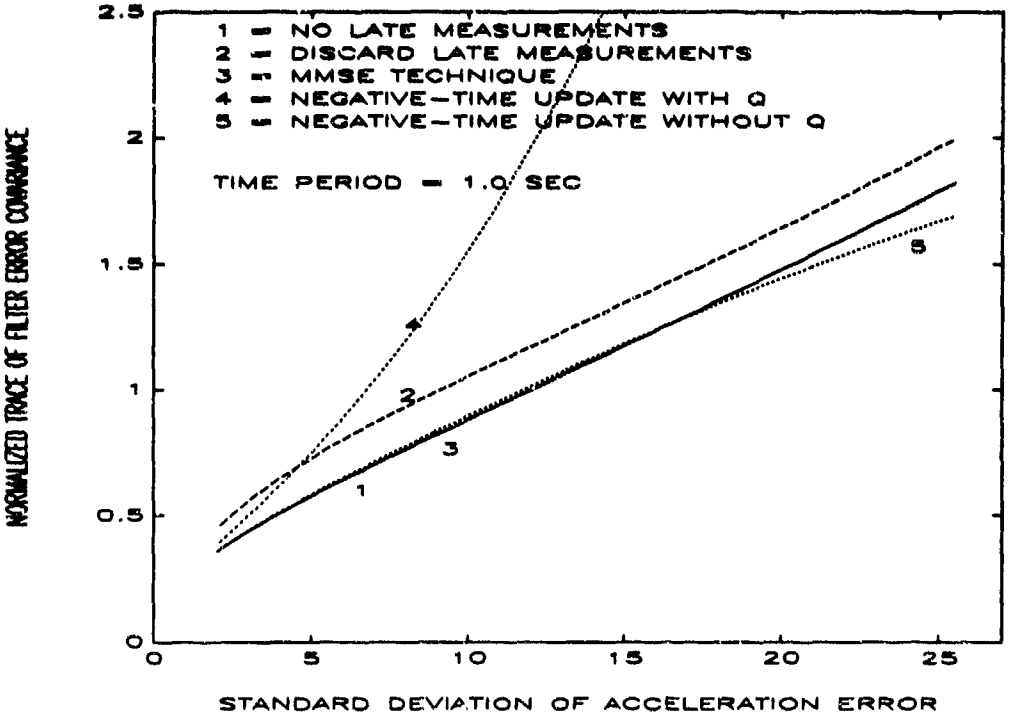

Figure 3–3. Negative-Time Update Technique Performance

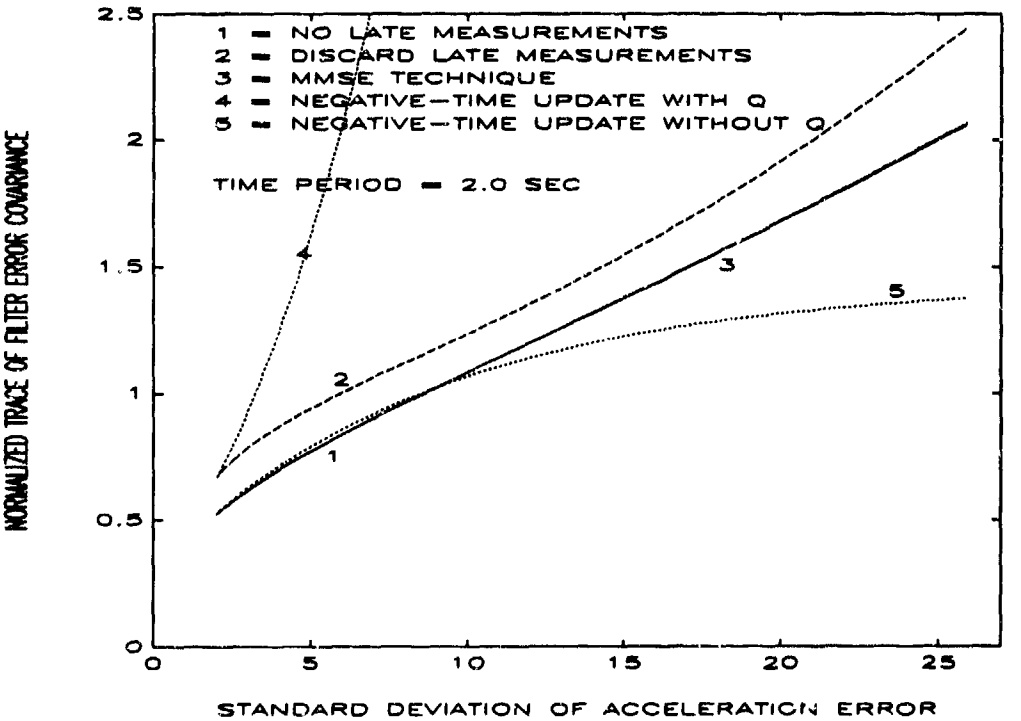

Figure 3–4. Negative-Time Update Technique Performance

CHAPTER 4

CEC APPROACH

This chapter interprets the *ad hoc* CEC-extended Kalman filter updating technique as specified in [1]. Analysis similar to that in the previous chapter is included for examination of the technique's performance.

CEC Specification For Negative-Time Updates

Assuming the same situation as in the previous chapter, a measurement arrives late with time tag, t_{k-1}, just after the extended Kalman filter update has been made for a measurement with time tag, t_k. This results in the time interval

$$T = t_{k-1} - t_k \tag{4.1}$$

From this point, noting $T < 0$, the standard filtering equations are used to make a backwards update with the exception that the plant noise is set to zero, (i.e., $Q(T) = 0$). The equations for this segment of the interpreted CEC negative-time update are given in the following equations.

Time Update:

$$X_{k-1|k-} = F(T)X_{k|k-} \tag{4.2}$$
$$P_{k-1|k-} = F(T)P_{k|k-}F^T(T) \tag{4.3}$$

Measurement Update:

$$X_{k-1|k} = X_{k-1|k-} + K_{k-1}[Z_{k-1} - h(X_{k-1|k-})] \tag{4.4}$$
$$P_{k-1|k} = [I - K_{k-1}H_{k-1}]P_{k-1|k-} \tag{4.5}$$
$$K_{k-1} = P_{k-1|k-}H_{k-1}^T[H_{k-1}P_{k-1|k-}H_{k-1}^T + R_{k-1}]^{-1} \tag{4.6}$$

After the state has been moved backwards and the state estimate, $X_{k-1|k}$, has been calculated, the state estimate is moved forward with the plant noise reintroduced by using the

absolute value of the negative-time interval to project forward to the current track valid time, t_k, to form $X_{k|k}$. This segment gives the time updates as

$$X_{k|k+} = F(|T|)X_{k-1|k} \tag{4.7}$$
$$P_{k|k+} = F(|T|)P_{k-1|k}F^T(|T|) + Q(|T|) \tag{4.8}$$

noting that now $Q(|T|)$ is nonzero and the time interval $|T| > 0$. Having predicted forward to the existing track valid time, t_k, the filter resumes normal operations on the next measurement.

Simple Numerical Example

A simple example that computes the covariance matrix is presented for comparison with the results of the previous example in Chapter 3. The following parameters were chosen to remain consistent with the previous example. Those parameters are given by

$$X_k = \begin{bmatrix} x \\ \dot{x} \end{bmatrix}_k \tag{4.9}$$
$$F_k(T) = \begin{bmatrix} 1 & T \\ 0 & 1 \end{bmatrix} \tag{4.10}$$
$$H_k = \begin{bmatrix} 1 & 0 \end{bmatrix} \tag{4.11}$$
$$R_k = 144.0 \tag{4.12}$$
$$\overline{q} = 5.0 \tag{4.13}$$

The initial covariance matrix is set to

$$P_{0|0} = \begin{bmatrix} 79 & 32 \\ 32 & 26 \end{bmatrix} \tag{4.14}$$

The CEC approach is used to calculate the error covariance matrix using (4.2)-(4.8) as discussed earlier. The final error covariance matrix results are

$$P_{4|4+} = \begin{bmatrix} 70.48 & 23.56 \\ 23.56 & 19.30 \end{bmatrix} \tag{4.15}$$

Recalling the results from the previous example found in Tables 3–1 and 3–2, a comparison of all four cases is presented in Table 4–1. It is noted that although the CEC *ad hoc* technique made a significant recovery from the negative-time interval, a nearly full recovery was not experienced as with the MMSE approach.

Table 4–1. Traces of Covariances $P_{4|4}$

CASE	TRACE
All measurements on time	82.376
Measurement Z_3 missing	105.734
Z_3 processed negative-time(MMSE)	82.376
Z_3 processed negative-time(CEC)	89.777

Negative-Time Updates and Constant Velocity Tracking

The program method used in the last section of Chapter 3 was used to evlauate the performance of the interpreted *ad hoc* CEC technique. The worst case scenario, where all late measurements are discarded and the sequential case where all measurements arrive on time, were compared with the CEC technique. The performance was again evaluated using a graph of the the normalized trace of the filter error covariance matrix versus the standard deviation of the acceleration error. Time periods of 0.25, 0.5, 1.0, and 2.0 sec were used in the evaluations. Figures 4–1 through 4–4 express the performance of the three techniques. The *ad hoc* CEC technique does not always perform better than the worst case scenario of discarding all late measurements. For longer time periods, the CEC technique was found to perform poorly, even with relatively small standard deviations of acceleration error, while the MMSE technique remained stable as shown in the previous chapter.

For each of the time periods used, the standard deviation of acceleration error at which the CEC technique breaks down was evaluated. Using (3.42), the corresponding tracking indexes were found in order to characterize the break down regions for the CEC technique. Figure 4–5 shows a plot of the tracking indexes at which the CEC technique fails versus the sample period. For a given sample period, the CEC technique will break-down for tracking index values greater than the value denoted by the line.

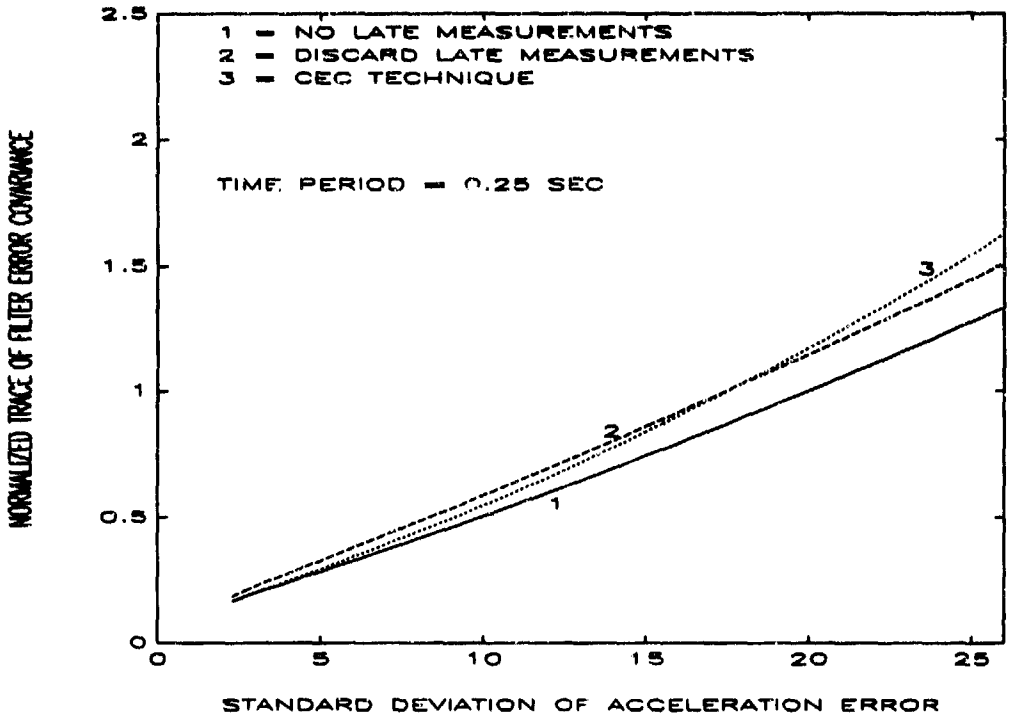

Figure 4–1. Negative-Time Update Technique Performance

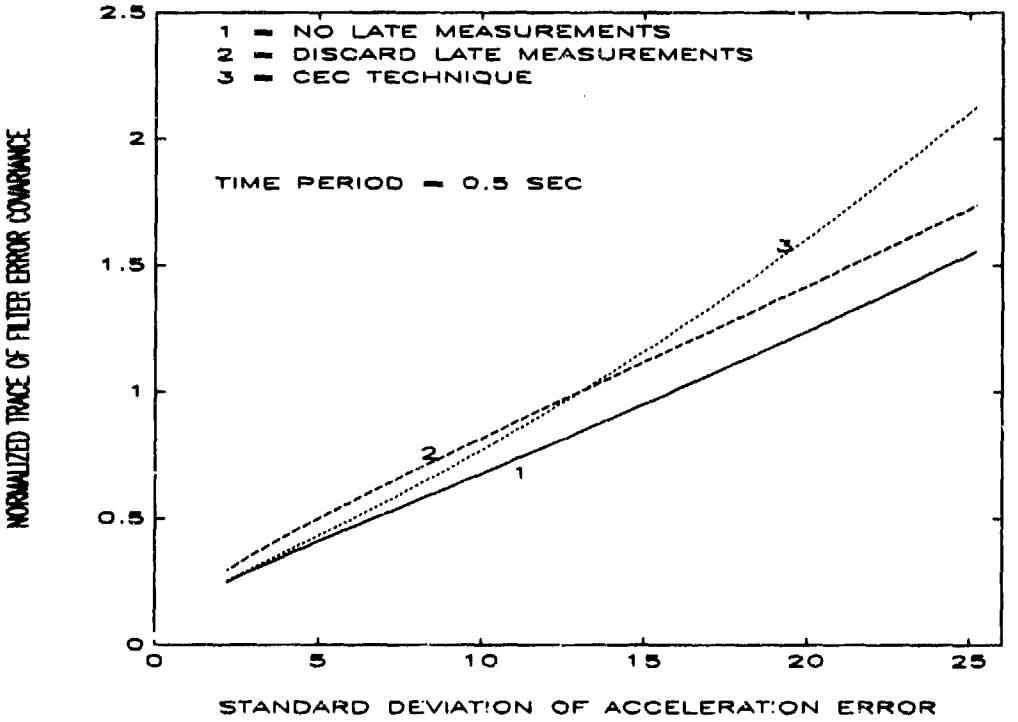

Figure 4–2. Negative-Time Update Technique Performance

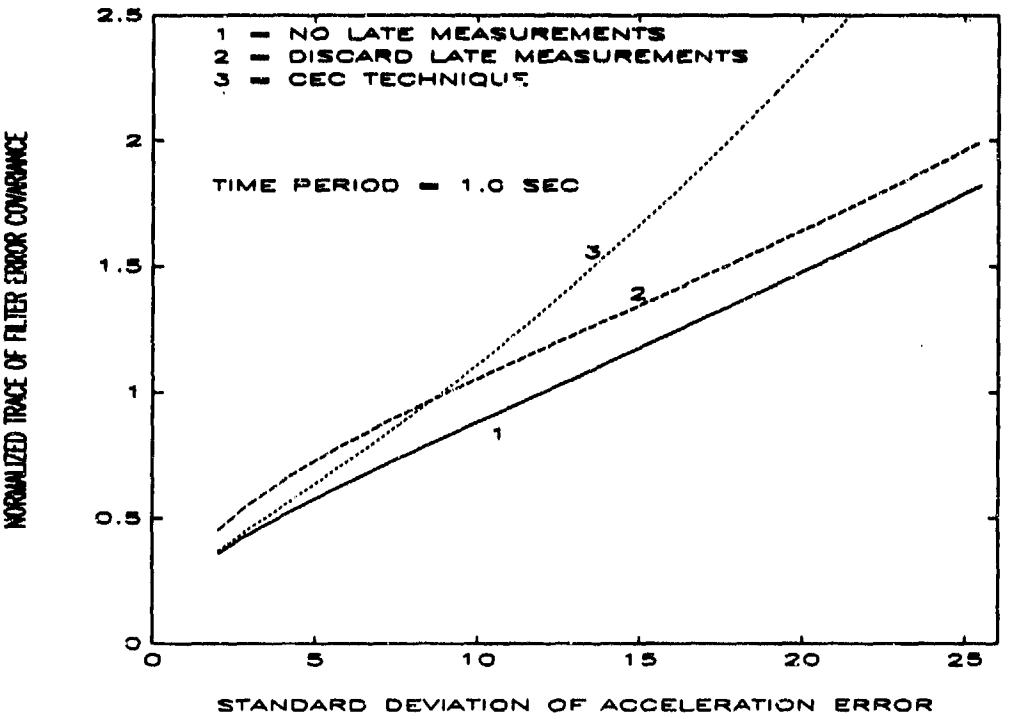

Figure 4–3. Negative-Time Update Technique Performance

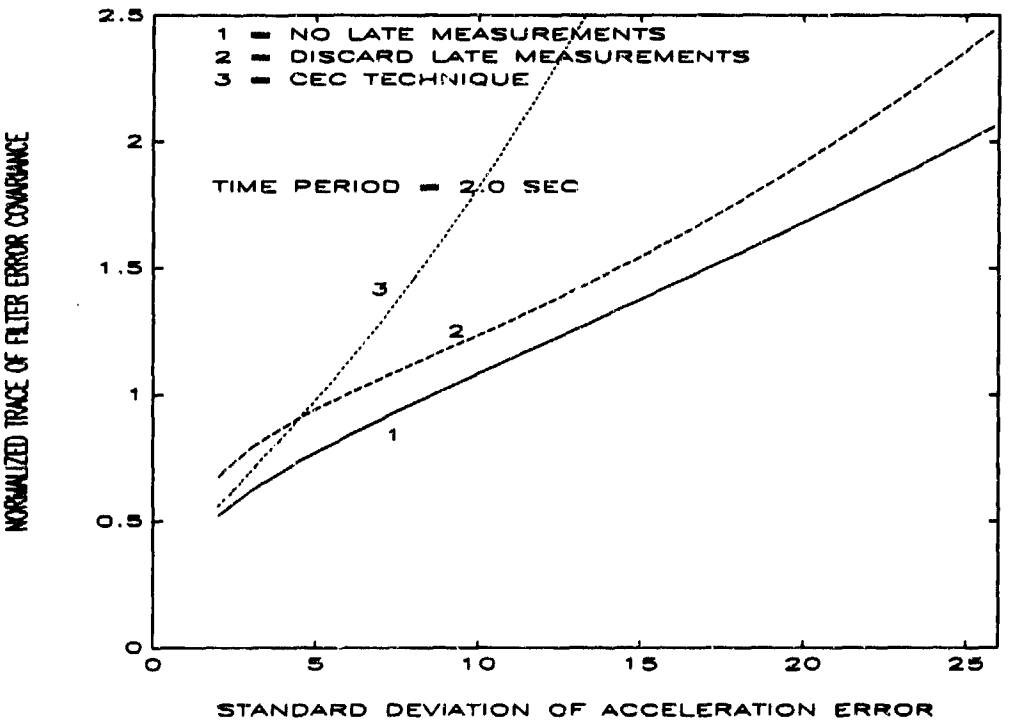

Figure 4–4. Negative-Time Update Technique Performance

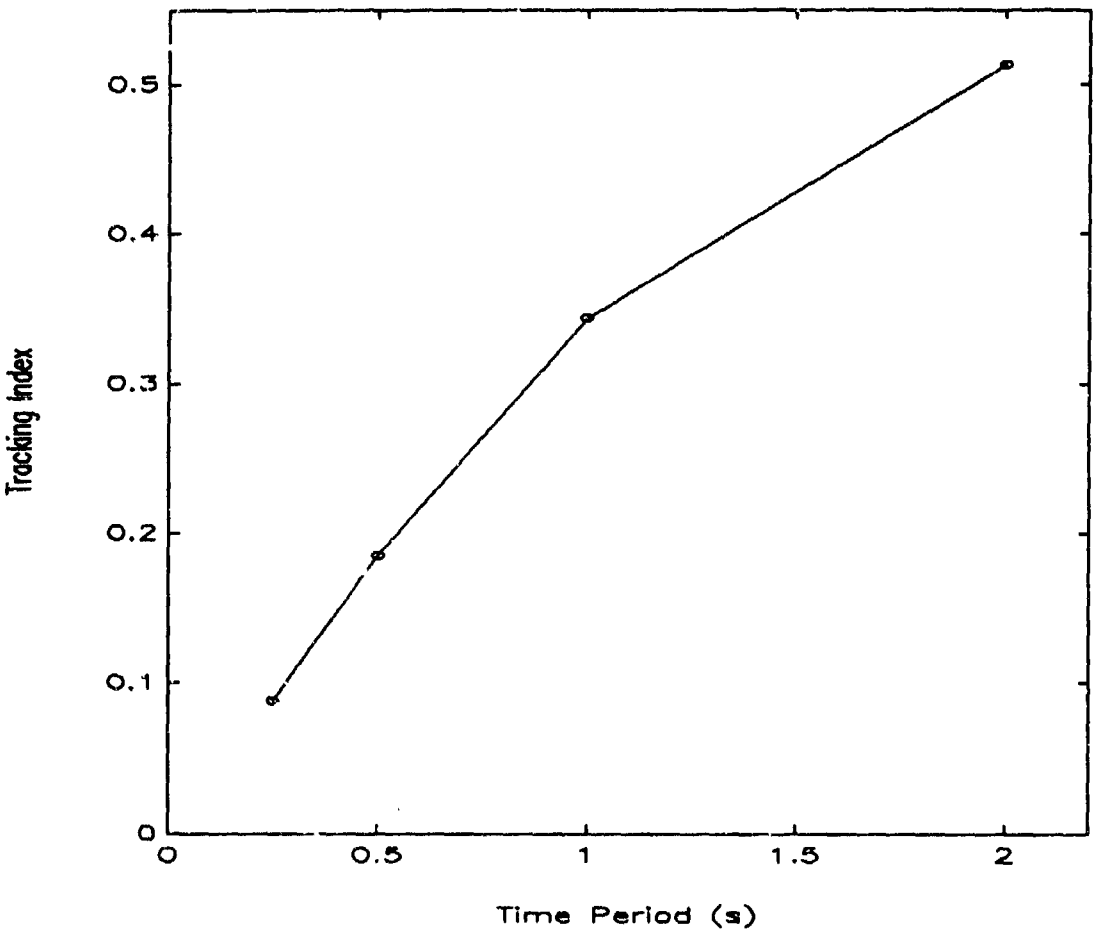

Figure 4–5. Tracking Index Break-Down Region for the CEC Technique

CHAPTER 5

SIMULATION RESULTS

The objective was to simulate an ownship sensor and a remote ship sensor tracking a common manuevering target with the remote ship transmitting its tracking data to ownship. This simulation enabled the performance of the interpreted CEC negative-time approach to be compared with the derived MMSE approach in a practical situation where data being transmitted from remote ship to ownship are delayed.

Simulation Setup

Figure 5–1 displays the scenario of the ships and target locations for this simulation. The ships are separated by 15 km along the x-axis making the remote ship coordinates with respect to the ownship reference frame,$(x, y, z) = (15, 0, 0)$ km. To simplify the simulation, motion between the two sensors was set to zero and the earth's shape was modeled to be locally flat. The flow chart in Figure 5–2 is a basic outline of the program operations. A single target trajectory, created using a trajectory generator program, was used for the simulation. A profile of the trajectory is found in Figure 5–3. The target has a constant altitude of 5 km. The target travels at Mach 2 for 44 sec making two 6g maneuvers between 12 and 21 sec and between 24 and 33 sec, respectively. When the target is not maneuvering, it maintains a constant velocity. The trajectory generated is in the form of a data matrix with even columns representing measurements from the ownship sensor and odd columns representing the measurements obtained by the remote ship sensor. The odd columns are offset by $(15, 0, 0)$ km, since every other measurement received by the ownship is a remote sensor measurement. Measurements from each sensor are received every 2 sec resulting in a received measurement every 1 sec when the data from each sensor are skewed in time.

The same trajectory was used in the simulation to study and test each of four cases. For the first case, the ownship uses its own measurements plus measurements from the remote ship to track the target, with all measurements arriving on time. The second case is similar to the first case except all the measurements received by the ownship from the remote ship are delayed and are discarded. The third case resembles the second, but the late measurements from the remote ship sensor are processed using the MMSE negative-time update approach derived in Chapter 3. In the fourth case, the delayed measurements received by the ownship from the remote ship are processed using the interpreted CEC approach of Chapter 4.

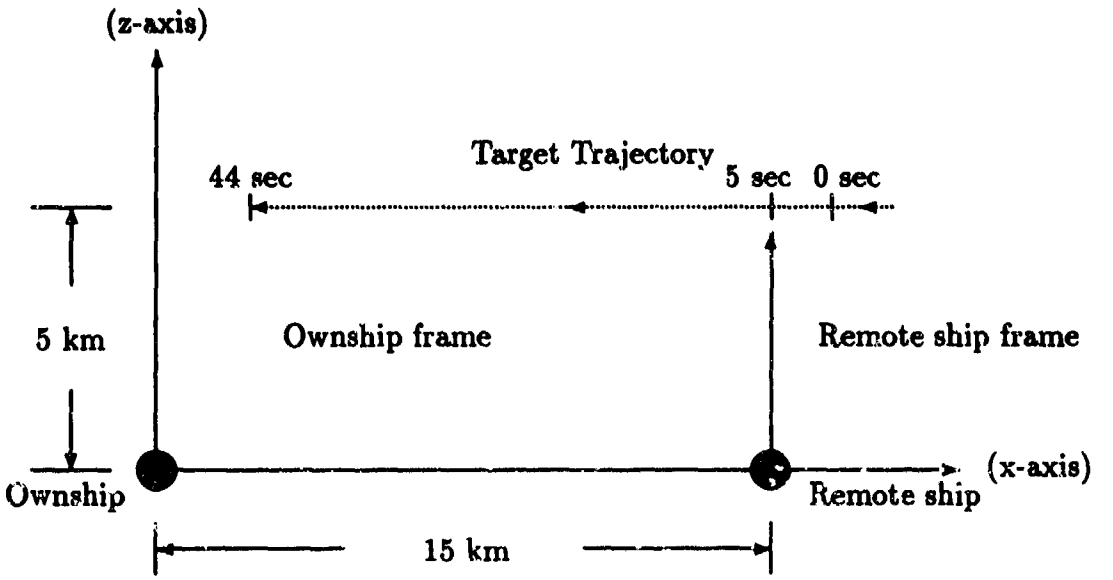

Figure 5–1. Profile of Ship and Target Locations

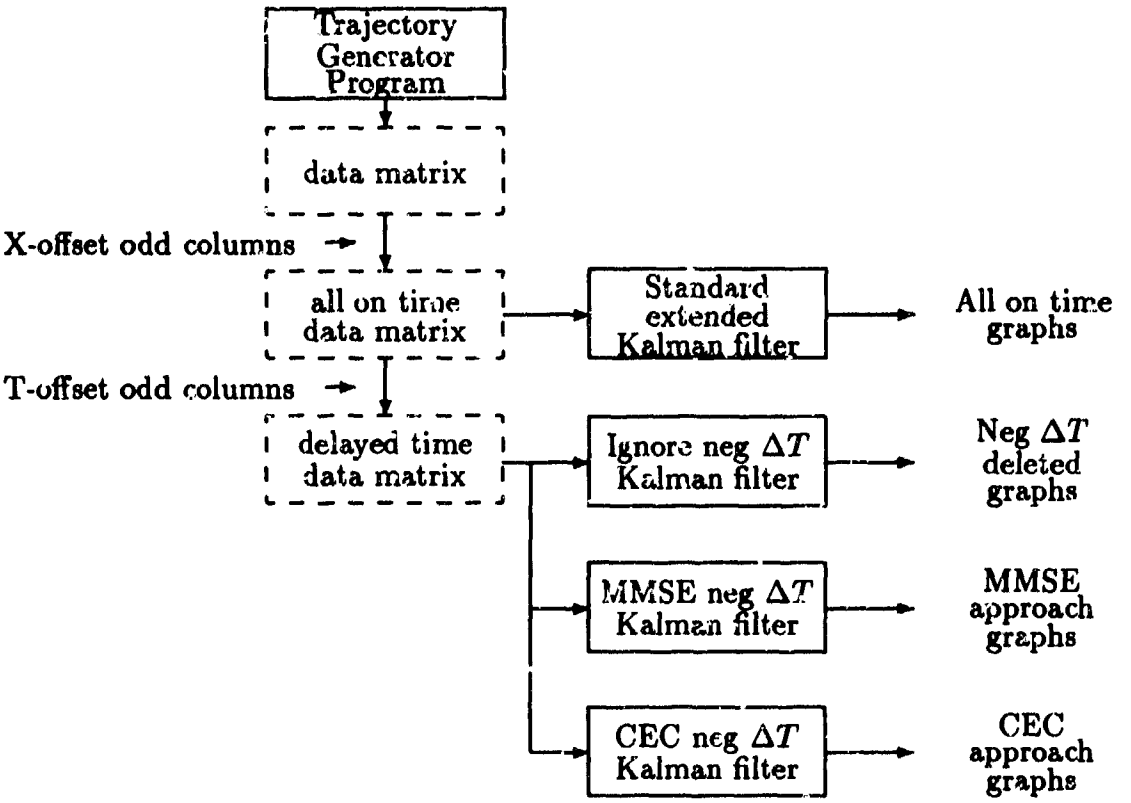

Figure 5–2. Basic Outline of Simulation

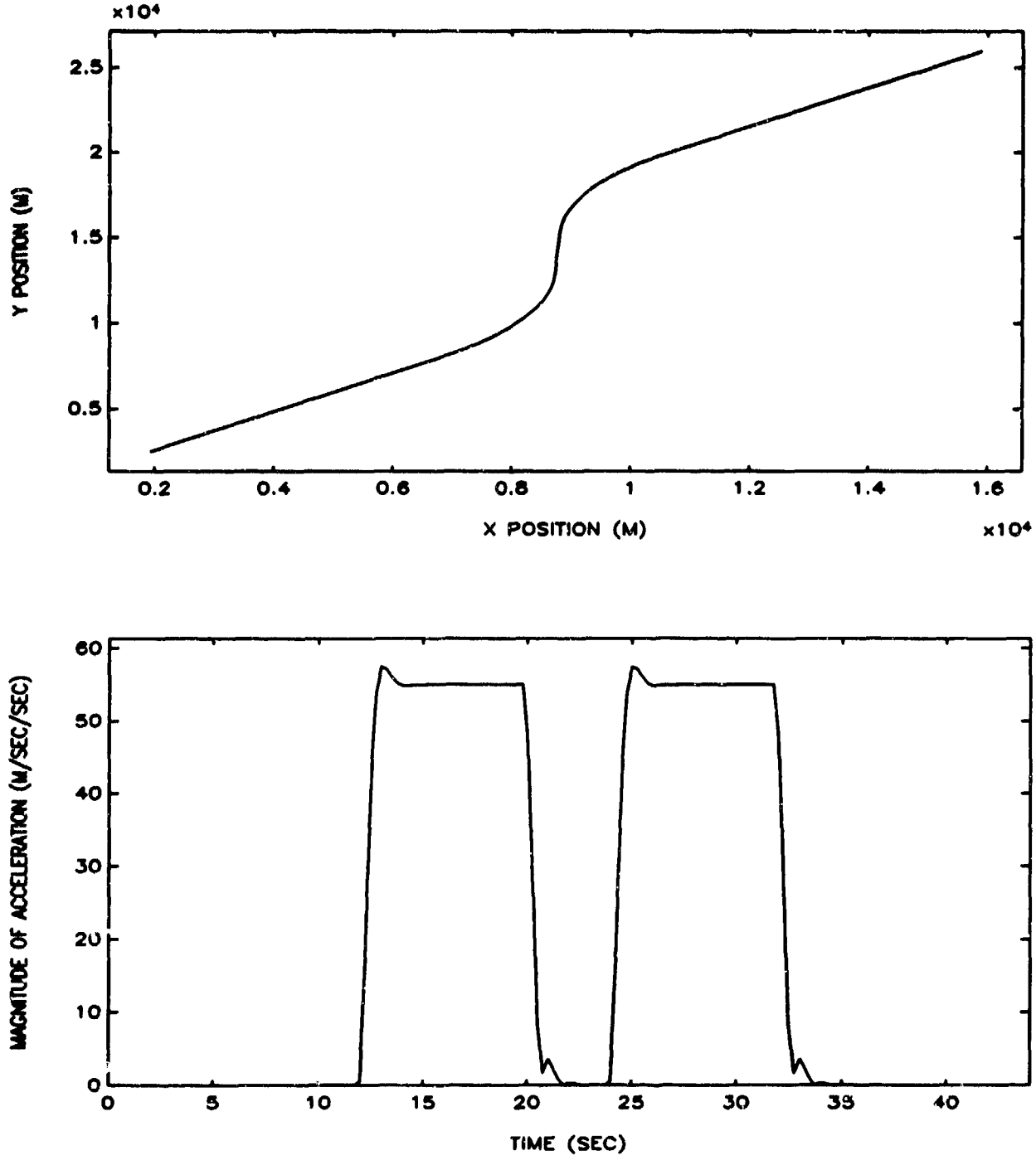

Figure 5-3. Profile of Target Trajectory

Results

The simulation output for each track filter is an average of 100 Monte Carlo experiments. The Root-Mean-Square-Errors (RMSE) in position and velocity are used to measure the performance of the negative-time update techniques implemented in the simulations. In the four cases, the combined measurements received from the two multiplatform sensors had a data rate of 1 Hz with a standard deviation in range of $\sigma_r = 12$ m, and standard deviation of angles $\sigma_b = \sigma_e = 2.5$ mrad. The arrival of measurements from the remote sensor are delayed slightly more than 1 sec. The results of the first three cases are given in Figure 5–4. The top and bottom graphs are an average RMSE of the position and velocity, respectively. Comparing the first two cases displays the improvement experienced with the concept of CEC, when all measurements from the remote sensor arrive on time, as opposed to using only the ownship sensor measurements. In the third case, the late measurements are processed using the MMSE negative-time update approach derived in Chapter 3. It is seen that the result is almost a complete recovery from the late measurements. The jagged lines that occur during the maneuvers for the case where all measurements arrive sequentially are the result of receiving data from multiple sensors with varying degrees of accuracy. Since the remote sensor is closer to the target than the ownship sensor, as shown in Figure 5–1, measurements from the remote sensor are better than the measurements from the ownship sensor. Since the measurements between ownship and remote are skewed in time, every other measurement being utilized will result in a better estimate. During the constant velocity portions of the track, this effect goes unnoticed, but during maneuvers where the mismatch of motion model is greater, the effect is seen. Since the MMSE approach does not compute a state estimate that corresponds to the measurement time of the remote sensor, RMSE were not computed at those times, and hence, the lines denoting the RMSE for the MMSE approach are not jagged. The results comparing the RMSE of position and velocity for cases three and four are found in Figure 5–5. Comparing the two techniques, it is seen that the CEC approach does result in a recovery from the late measurements, but the results are not as precise as the recovery experienced from the MMSE approach.

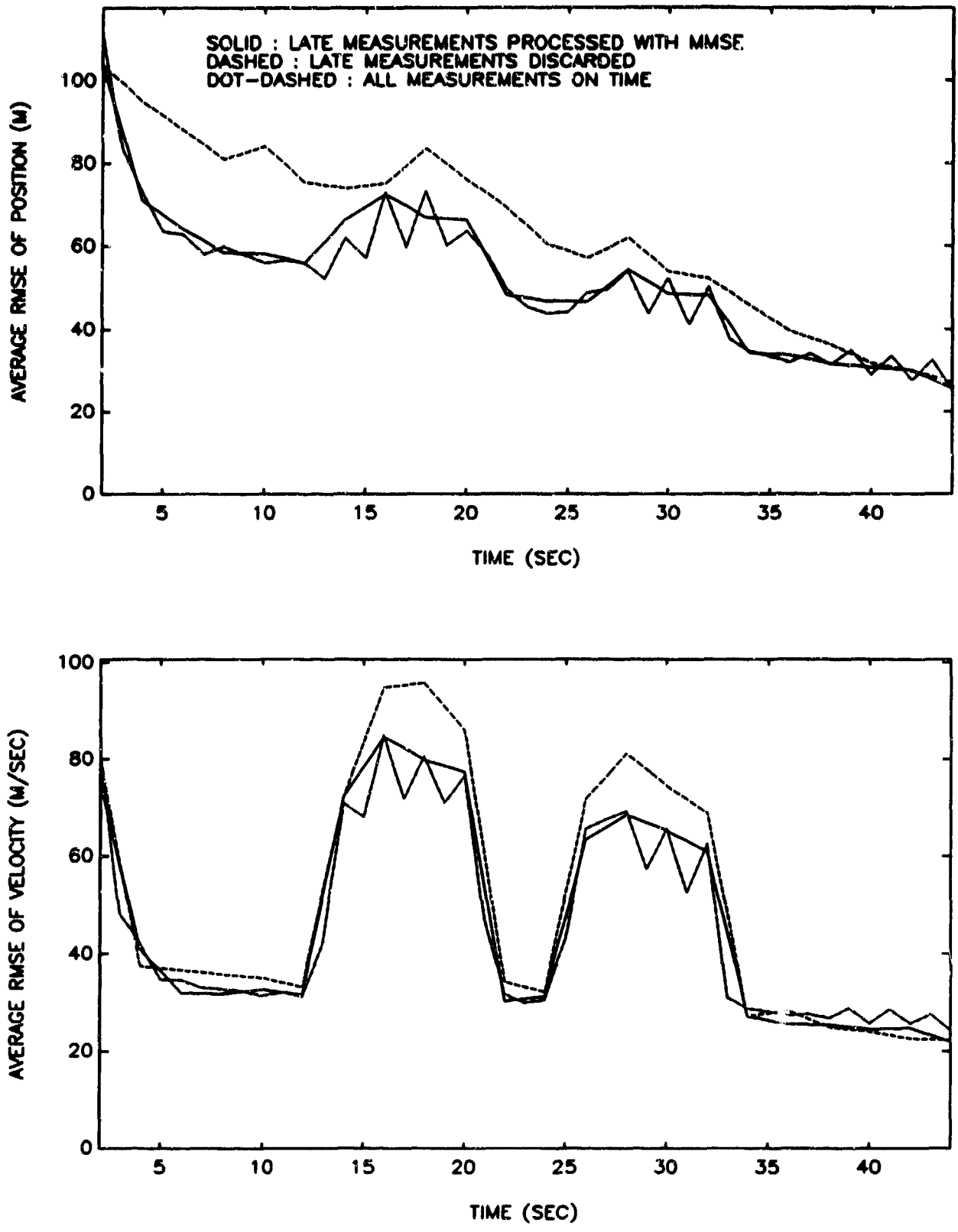

Figure 5–4. Tracking Results for Cases 1-3

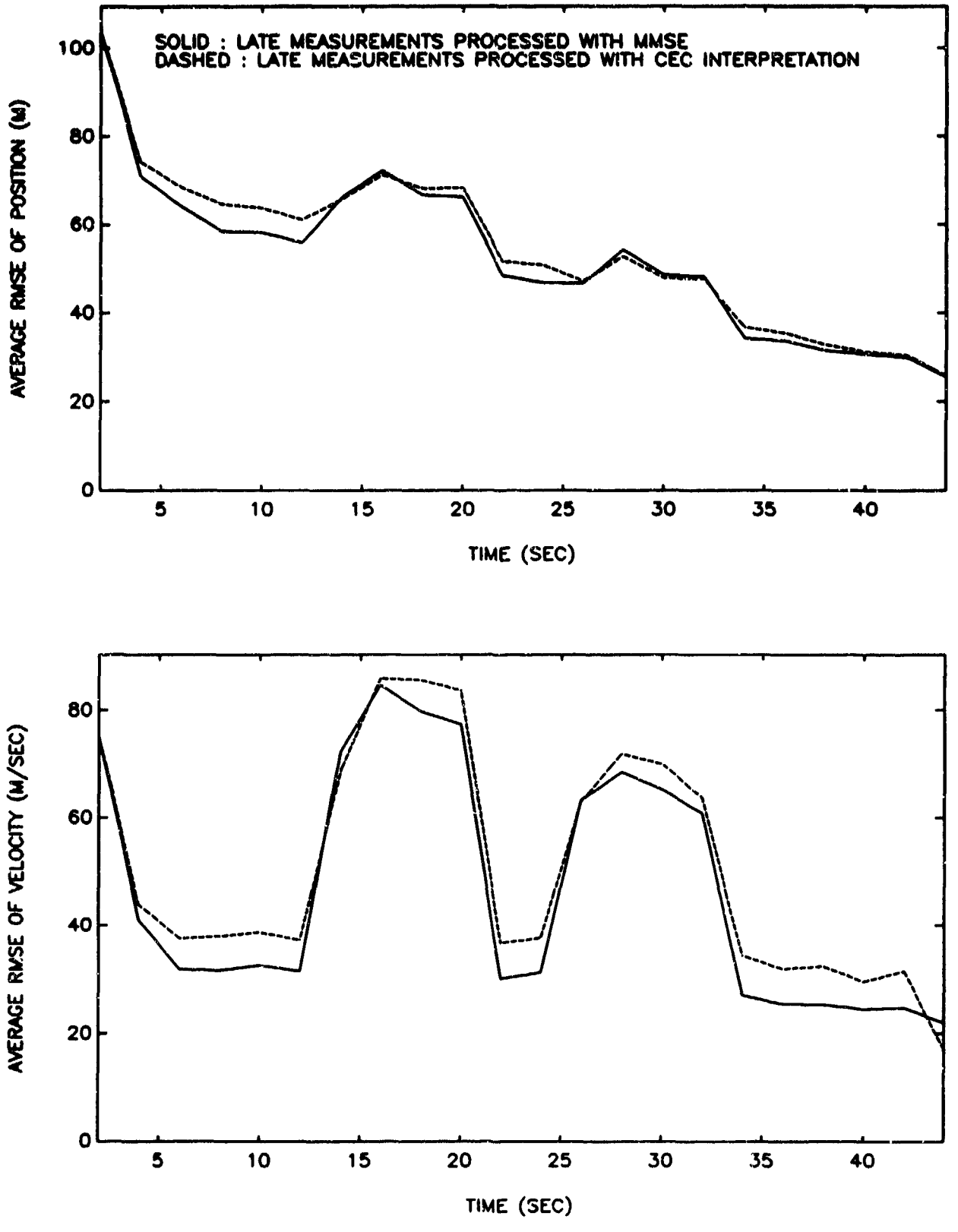

Figure 5–5. Tracking Results for Cases 3 and 4

CHAPTER 6

CONCLUSIONS

An MMSE approach for processing time delayed data was developed and compared with other techniques for processing time delayed data. One of those techniques for processing negative-time data uses the plant noise Q_k throughout the entire negative-time update interval (Q-on). Analysis of the Q-on technique showed that it is unstable and performs very poorly. Another technique involved setting Q_k to zero throughout the entire negative-time update interval (Q-off). Analysis of the Q-off technique showed that it performs better than the Q-on technique, but for larger levels of plant noise and longer time intervals the filter covariance is "too good" in that it is smaller than that achieved by sequential processing of the data (all measurements on time). The interpreted CEC approach was found to a be more desirable approach to negative-time updates than either the Q-on or Q-off technique. However, when the MMSE approach was compared with the CEC approach, the CEC approach was found to be the inferior technique. The CEC approach may have problems when used with filters designed for highly maneuvering targets at low data rates, while the MMSE approach is rather stable with respect to levels of plant noise and sample periods.

The possibility of experiencing delayed data causing negative-time intervals has added complexity to the CEC concept. More analysis of the issues associated with negative-time updates is desirable. Issues revolving around the negative-time update that need to be studied include status of target maneuvers, data association in the presence of clutter and false alarms, and an on-line technique to assess the value added if a negative-time measurement is utilized. This study involved only a constant velocity Kalman filter. Other problems could arise if other tracking techniques such as multiple model filtering are used. For example, at the beginning of a target maneuver, a multiple model filter may undergo a model change just prior to receiving negative-time data. In this situation it would be useful to have a method for deciding which model would be used for processing the negative-time data. Also, an on-line technique is needed for evaluating the need and benefit of using delayed data during a tracking process. In a situation where good data on a target has been attained recently, the delayed data can be ignored, while on the other hand, if very little data on the target have been attained recently, the delayed data may be critical to maintaining a good track.

REFERENCES

1. *Software Requirements Specification (SRS) for the Cooperative Engagement Capability (CEC)*, Naval Sea Systems Command, Department of the Navy, Weapons Specification WS-32892.

2. Thomopoulis, C. A. and Zhang, L., "Distributed Filtering with Random Sampling and Delay," *Proceedings of SPIE Sensor Fusion*, SPIE Vol. 931, Orlando, FL, 1988.

3. Bar-Shalom, Y. and Fortman, T. E., *Tracking and Data Association*, Academic Press Inc., Orlando, FL, 1988.

4. Gelb, A., ed., *Applied Optimal Estimation*, The M.I.T. Press, Cambridge, MA, 1979.

APPENDIX A

NOTE ON F. R. CASTELLA'S MULTI-SITE, MULTI-SENSOR TRACKING FILTER

The proposed tracking algorithm described in this appendix first appears in the Applied Physics Laboratory internal memorandum F2A-92-1-002 dated 16 January 1992. Its principle features are as follows:

(1) A discrete time Kalman filter with state vector

$$\mathbf{X} = \begin{bmatrix} x & \dot{x} & y & \dot{y} & z & \dot{z} \end{bmatrix}^T$$

and a constant velocity model $\Phi(T)$ is used.

(2) Measurements from various sites, including ownship, are received for processing. A given measurement may come from one of several types of sensors. One may be from a radar that can measure elevation but not doppler, whereas another may come from a radar that can measure doppler, but not elevation.

(3) Measurements M_k arrive as "raw data"; that is, individual measured parameters such as bearing or slant range each appear accompanied by a time stamp, a standard deviation, sensor location (as latitude-longitude), and sensor ship's heading, pitch and roll as required. The Kalman updates are accomplished one measured parameter at a time with an appropriate output matrix H_k computed for each measured parameter at each update.

(4) Each Kalman filter within the Cooperative Engagement System operates from the point of view of a local, stabilized (x_1, y_1, z_1) coordinate system. Data from other sensors are referenced to a remote, stabilized coordinate system (x_2, y_2, z_2) with a known, remote latitude-longitude.

(5) The Kalman filter with its state $\mathbf{X} \in \mathcal{R}^6$ has the usual covariance matrix $P \in \mathcal{R}^{6\times6}$ representing accumulated measurement errors and plant noise. There also is a measurement-noise-only covariance matrix $P_S \in \mathcal{R}^{6\times6}$ that is carried to facilitate decision processes outside the Kalman filter proper. The matrix P_S does not otherwise affect the operation of the filter.

The Kalman filter equations used are stated below. The notation used here is $\mathbf{X}_{k|k-1}$ for projected state (as opposed to $\delta\hat{\underline{x}}$ used originally) and $\mathbf{X}_{k|k}$ for filtered state (as opposed to $\delta\tilde{\underline{x}}$ in the original). [1]

$$\mathbf{X}_{k|k-1} = \Phi(T)\mathbf{X}_{k-1|k-1} \quad \text{(A.1)}$$

$$P_{k|k-1} = \Phi(T)P_{k-1|k-1}\Phi(T)^T + Q_k \quad \text{(A.2)}$$

$$P_{S,k|k-1} = \Phi(T)P_{S,k-1|k-1}\Phi(T)^T \quad \text{(A.3)}$$

$$K_k = P_{k|k-1}H_k^T(H_kP_{k|k-1}H^T + R_k)^{-1} \quad \text{(A.4)}$$

$$\mathbf{X}_{k|k} = \mathbf{X}_{k|k-1} + K_k[M_k - M_p(\mathbf{X}_{k|k-1})] \quad \text{(A.5)}$$

$$P_{k|k} = (I - K_kH_k)P_{k|k-1} \quad \text{(A.6)}$$

[1] The original document treats state as $\underline{x}(0)$, the state at track initiation, plus a summation of incremental corrections $\delta\underline{x}_k$. This convention is not used here.

$$P_{S,k|k} = (I - K_k H_k) P_{S,k|k-1} (I - K_k H_k)^T + K_k R_k K_k^T \tag{A.7}$$

The specific means by which these Kalman filter equations are employed to effect track filtering will now be explored.

Plant Model and Plant Noise

Since the Cooperative Engagement Processor (CEP) tracking algorithm is a constant-velocity Kalman filter, the transition model for the chosen state vector $\mathbf{X}$ is given by

$$\Phi(T) = \begin{bmatrix} 1 & T & 0 & 0 & 0 & 0 \\ 0 & 1 & 0 & 0 & 0 & 0 \\ 0 & 0 & 1 & T & 0 & 0 \\ 0 & 0 & 0 & 1 & 0 & 0 \\ 0 & 0 & 0 & 0 & 1 & T \\ 0 & 0 & 0 & 0 & 0 & 1 \end{bmatrix} \tag{A.8}$$

where T is the time increment between updates.

In this particular realization, measurements M_k are each scalars that reflect some predicted function of the state vector $M_p(\mathbf{X})$, rather than just one of the elements of $\mathbf{X}$. The 'innovation' (the bracketed term of (A.5) above) is now the difference between measurement M_k and 'predicted' $M_p(\mathbf{X}_{k|k-1})$. Thus, the measurement matrix H_k^p becomes a row vector of partial derivatives given by

$$H_k^p = \begin{bmatrix} \dfrac{\partial M_p}{\partial x} & \dfrac{\partial M_p}{\partial \dot{x}} & \dfrac{\partial M_p}{\partial y} & \dfrac{\partial M_p}{\partial \dot{y}} & \dfrac{\partial M_p}{\partial z} & \dfrac{\partial M_p}{\partial \dot{z}} \end{bmatrix} \tag{A.9}$$

evaluated at $\mathbf{X}_{k|k-1}$.

The plant noise Q_k is represented by the formulation

$$Q_k = \begin{bmatrix} \mathbf{q}_1 & 0_{2\times 2} & 0_{2\times 2} \\ 0_{2\times 2} & \mathbf{q}_2 & 0_{2\times 2} \\ 0_{2\times 2} & 0_{2\times 2} & \mathbf{q}_3 \end{bmatrix} \tag{A.10}$$

$$\mathbf{q}_i = q_i \begin{bmatrix} \dfrac{T^3}{3} & \dfrac{T^2}{2} \\ \dfrac{T^2}{2} & T \end{bmatrix}, \quad i = 1, 2, 3 \tag{A.11}$$

$$0_{2\times 2} = \begin{bmatrix} 0 & 0 \\ 0 & 0 \end{bmatrix} \tag{A.12}$$

Each scalar q_i is a plant noise spectral density in units of length^2/time^3 = acceleration^2/Hz. This parameter will be supplied based upon a separate determination of the existence of a target maneuver. Further details of maneuver detection and acceleration estimation are not given in the memorandum under discussion and must be treated in further commentary notes.

Coordinate Systems

With the role of the CEP tracking algorithm being to accept measurements from many different sensors at many different locations, coordinate conversion plays a very important part in its formulation. This section will set out coordinate system notation conventions, drawings of the various coordinate systems, and the relationships used to express measurements that are made in one system in terms of another.

Figure A–1 illustrates worldwide coordinate systems expressed in longitude L (positive L $\Rightarrow$ East from Prime Meridian), latitude μ (positive $\mu \Rightarrow$ North from the Equator), and in the earth-centered rectangular coordinate system $(\hat{x}_0, \hat{y}_0, \hat{z}_0)$. Any vector $\overline{R}_i$ can be expressed as an earth-centered vector (x_0, y_0, z_0) in terms of L_i, μ_i, and its length $|R_i|$ by the well-known relationship

$$\overline{R}_i = \begin{bmatrix} x_0 \\ y_0 \\ z_0 \end{bmatrix} = |R_i| \begin{bmatrix} \cos L_i \cos \mu_i \\ \sin L_i \cos \mu_i \\ \sin \mu_i \end{bmatrix} \tag{A.13}$$

In Figure A–1, the head of vector R_i is shown as the origin for a 'stabilized' coordinate system $(\hat{x}_i, \hat{y}_i, \hat{z}_i)$; that is, one for which $\hat{x}$ is local East, $\hat{y}_i$ is local North, and $\hat{z}_i$ is local vertical. In the CEP tracker, $\overline{R}_1$ points to ownship and state estimate $\hat{X}$ is maintained in the $(\hat{x}_1, \hat{y}_1, \hat{z}_1)$ coordinate system. Measurements received from another ship located at (L_2, μ_2) and at the head of vector $\overline{R}_2$ may have been made in either stabilized local coordinates as (x_2, y_2, z_2) or in 'deck coordinates' as (x_2''', y_2''', z_2''') having the same origin.

Figure A–2 illustrates the relationships among earth-centered coordinates (x_0, y_0, z_0), local stabilized coordinates (x_1, y_1, z_1), and remote stabilized coordinates (x_2, y_2, z_2). An ownship sensor makes measurements on a target in terms of vector $\overline{T}_1$, while a remote sensor makes measurements on the same target in terms of vector $\overline{T}_2$. The vector displacement between remote and local coordinates in earth-centered (x_0, y_0, z_0) is

$$\Delta R_0 = \overline{R}_1 - \overline{R}_2 = \begin{bmatrix} |R_1| \cos \mu_1 \cos L_1 - |R_2| \cos \mu_2 \cos L_2 \\ |R_1| \cos \mu_1 \sin L_1 - |R_2| \cos \mu_2 \sin L_2 \\ |R_1| \sin \mu_1 - |R_2| \sin \mu_i \end{bmatrix}_0 \tag{A.14}$$

The well-known matrix

$$M^{(i0)} \triangleq \begin{bmatrix} -\sin L_i & \cos L_1 & 0 \\ -\sin \mu_i \cos L_i & \sin \mu_i \sin L_i & \cos \mu_i \\ \cos \mu_i \cos L_i & \cos \mu_i \sin L_i & \sin \mu_i \end{bmatrix} \tag{A.15}$$

rotates any vector (x_0, y_0, z_0) into the i-th coordinate system from the earth-centered system. Coordinate rotation in the opposite direction is achieved via the inverse matrix

$$M^{(0i)} = [M^{(i0)}]^{-1} = [M^{(i0)}]^T \tag{A.16}$$

which is equal to the transpose since these matrices are unitary. Thus, the displacement between local (x_1, y_1, z_1) and remote (x_2, y_2, z_2) in local coordinates is

$$\Delta R_1 = M^{(10)} \Delta R_0 \tag{A.17}$$

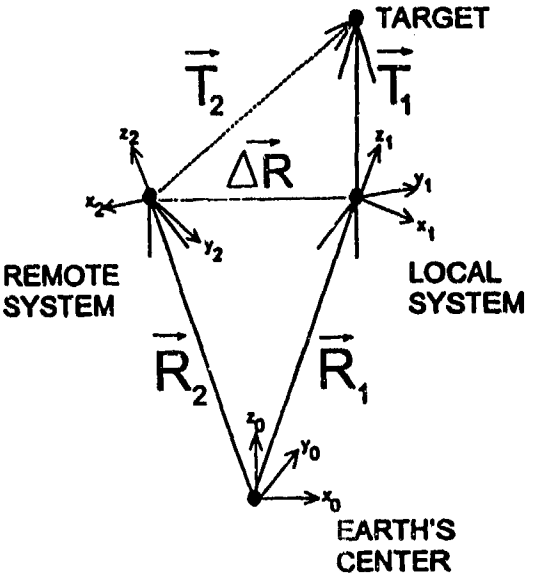

Figure A–1. Longitude L, Latutude μ, and Earth-Centered Unit Vectors $(\hat{x}_0, \hat{y}_0, \hat{z}_0)$

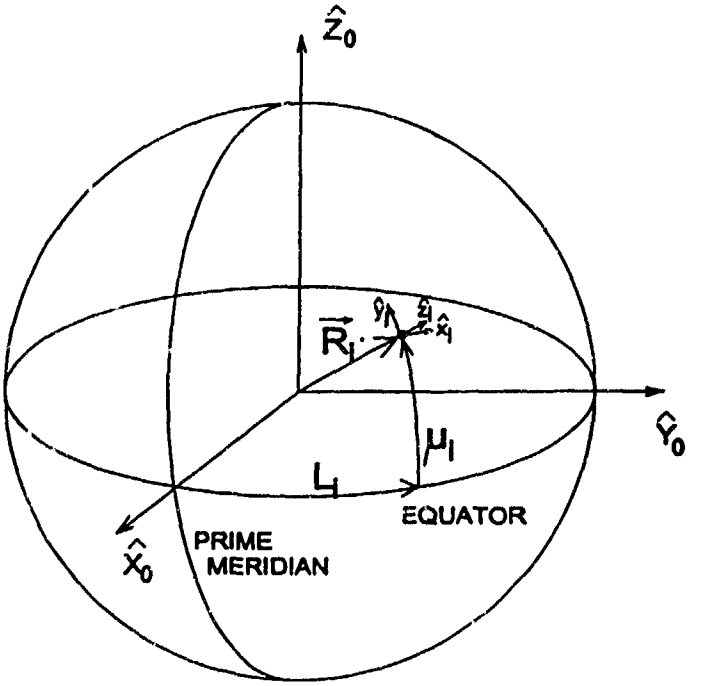

Figure A–2. Local and Remote Coordinate Systems of the CEP Tracker

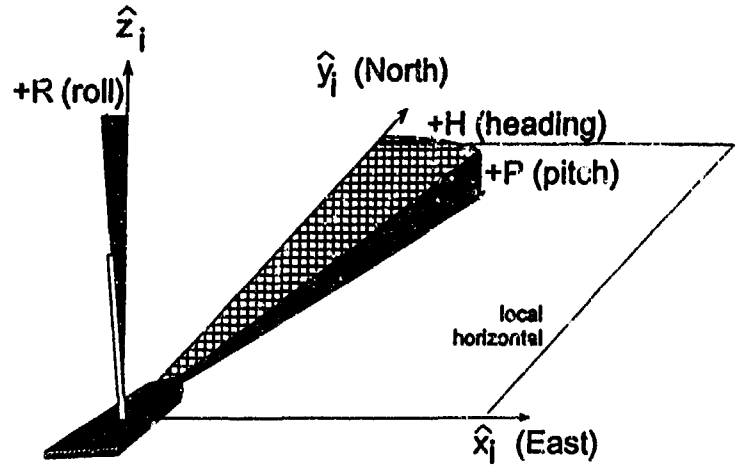

Figure A–3. Converting Stabilized Coordinates to Deck Coodinates

Hence, any attribute of a target measured in terms of vector $\overline{T}_2$ by a remote sensor at (L_2, μ_2) as stabilized (x_2, y_2, z_2) is expressable in terms of the ownship system state vectors

$$\begin{bmatrix} x_2 \\ y_2 \\ z_2 \end{bmatrix} = M^{(20)} M^{(01)} \left(\begin{bmatrix} x_1 \\ y_1 \\ z_1 \end{bmatrix} + \Delta R_1 \right) \tag{A.18}$$

Some ship sensors, such as the SPY-1, will produce their measurements in stabilized coordinates ($\hat{x}$ as East, etc.), while others, such as the SPS-49, report in 'deck coordinates' ($\hat{y}'''$ is toward the bow of the ship). Figure A–3 illustrates the three angles by which a stabilized system is rotated into a deck system. The Navy convention for coordinate rotation differs from the mathematical convention in the order and in the sign convention of the individual rotations. In the Navy convention, positive angles represent clockwise rotations. In going from the stabilized system (x_i, y_i, z_i) to the deck oriented system (x_i''', y_i''', z_i'''), one first rotates about z_i by heading h_i (which is positive for clockwise from North) into (x_i', y_i', z_i') by way of

$$\begin{bmatrix} x_i' \\ y_i' \\ z_i' \end{bmatrix} = H^{(i)} \mathbf{X}_i = \begin{bmatrix} \cos h_i & -\sin h_i & 0 \\ \sin h_i & \cos h_i & 0 \\ 0 & 0 & 1 \end{bmatrix} \begin{bmatrix} x_i \\ y_i \\ z_i \end{bmatrix} \tag{A.19}$$

Secondly, one rotates about x_i' by the pitch angle p_i (which is positive for the bow going down) to get into (x_i'', y_i'', z_i'') by way of

$$\begin{bmatrix} x_i'' \\ y_i'' \\ z_i'' \end{bmatrix} = P^{(i)} \mathbf{X}_i' = \begin{bmatrix} 1 & 0 & 0 \\ 0 & \cos p_i & -\sin p_i \\ 0 & \sin p_i & \cos p_i \end{bmatrix} \begin{bmatrix} x_i' \\ y_i' \\ z_i' \end{bmatrix} \tag{A.20}$$

Finally, one rotates about y_i'' by roll angle r_i (which is positive for roll to portside) into the final deck system (x_i''', y_i''', z_i''') by way of

$$\begin{bmatrix} x_i''' \\ y_i''' \\ z_i''' \end{bmatrix} = R^{(i)}\mathbf{X}_i'' = \begin{bmatrix} \cos r_i & 0 & \sin r_i \\ 0 & 1 & 0 \\ -\sin r_i & 0 & \cos r_i \end{bmatrix} \begin{bmatrix} x_i'' \\ y_i'' \\ z_i'' \end{bmatrix} \tag{A.21}$$

Thus measurements made by an ownship sensor in deck coordinates are expressed in ownship stable coordinates as

$$\begin{bmatrix} x_1''' \\ y_1''' \\ z_1''' \end{bmatrix} = R^{(1)}P^{(1)}H^{(1)} \begin{bmatrix} x_1 \\ y_1 \\ z_1 \end{bmatrix} \tag{A.22}$$

and a remote sensor using deck coordinates makes measurements expressed in ownship stable coordinates as

$$\begin{bmatrix} x_2''' \\ y_2''' \\ z_2''' \end{bmatrix} = R^{(2)}P^{(2)}H^{(2)}M^{(20)}M^{(01)} \left(\begin{bmatrix} x_1 \\ y_1 \\ z_1 \end{bmatrix} + \Delta R_1 \right) \tag{A.23}$$

For convenience, the following products of coordinate rotation matrices will be designated.

$$U \triangleq R^{(1)}P^{(1)}H^{(1)} \tag{A.24}$$

$$N \triangleq M^{(20)}M^{(01)} \tag{A.25}$$

$$V \triangleq R^{(2)}P^{(2)}H^{(2)}N \tag{A.26}$$

Measurement Functions M_p and Matrices H

The CEP tracking algorithm is configured to handle four kinds of measurements from two different kinds of sensor (radars), neither of which alone can make all four kinds of measurements. One kind of radar, the SPY-1 type, produces measurements in local stabilized coordinates whereas other types, bearing-only sets, produce their results in deck coordinates. Moreover, a given processor my be resident on a ship having either type of set. The measurement types are

Bearing

Slant range

Elevation

Doppler

In order to process the parameter M_k characteristic of each kind of measurement, the following steps must be undertaken.

(1) Evaluate $M_p(\mathbf{X}_{k|k-1})$ for *predicted* parameter.

(2) Evaluate the partial derivatives needed to complete matrix H_k^p.

(3) Execute the Kalman filter formulas (A–1) through (A–7).

The formulas needed to carry out Steps (1) and (2) will now be discussed.

Formulas for $M_p(\mathbf{X})$ and $\frac{\partial M_p}{\partial c}$, $c = x, \dot{x}, y, \dot{y}, z, \dot{z}$, for each measurement type are given in Tables A–1 through A–4. Table A–1 gives $M_p(\mathbf{X})$ and $\frac{\partial M_p}{\partial c}$ for processing local stabilized coordinates (x_1, y_1, z_1), while Table A–2 gives those results for local deck coordinates (x_1''', y_1''', z_1'''). Table A–3 gives $M_p(\mathbf{X})$ and $\frac{\partial M_p}{\partial c}$ for processing remote stabilized coordinates (x_2, y_2, z_2), while Table A–4 gives those results for remote deck coordinates (x_2''', y_2''', z_2'''). As an example of these formulas' derivations, the bearing measurement will be treated in detail.

Bearing in Local Stabilized Coordinates

While bearing may be defined in terms of the tangent function $\tan B_1 = \left(\frac{x_1}{y_1}\right)$, in using the inverse $B_1 = \tan^{-1}\left(\frac{x_1}{y_1}\right)$ the programmer must, of course, make provisions for cases where $y_1 \leq 0$. Since these provisions involve adding a constant to $B_1(x_1, y_1)$, the formulas for partial derivatives need no such modifications.

Using the general formulation for the derivative of $\tan^{-1}$,

$$\frac{\partial}{\partial x_1} \tan^{-1}\left(\frac{u}{v}\right) = \frac{v\frac{\partial u}{\partial x_1} - u\frac{\partial v}{\partial x_1}}{u^2 + v^2} \tag{A.27}$$

With $u = x_1$ and $v = y_1$ it follows immediately that

$$\frac{\partial}{\partial x_1} B_1 = \frac{y_1}{x^2 + y^2} \tag{A.28}$$

and that

$$\frac{\partial}{\partial y_1} B_1 = \frac{-x_1}{x^2 + y^2} \tag{A.29}$$

Bearing in Local Deck Coordinates

Now bearing is defined by

$$\tan B_1''' = \frac{x_1'''}{y_1'''} \tag{A.30}$$

Using the coordinate rotation matrix $U \triangleq [U_{ij}]$ of (A.24), x_1''' and y_1''' are found to be

$$x_1''' = \begin{bmatrix} 1 & 0 & 0 \end{bmatrix} U \begin{bmatrix} x_1 \\ y_1 \\ z_1 \end{bmatrix} \tag{A.31}$$

$$= x_1 U_{11} + y_1 U_{12} + z_1 U_{13} \tag{A.32}$$

and

$$y_1''' = \begin{bmatrix} 0 & 1 & 0 \end{bmatrix} U \begin{bmatrix} x_1 \\ y_1 \\ z_1 \end{bmatrix} \tag{A.33}$$

$$= x_1 U_{21} + y_1 U_{22} + z_1 U_{23} \tag{A.34}$$

Again using (A.27) with $u = x_1'''$ and $v = y_1'''$ the derivatives become

$$\frac{\partial B_1'''}{\partial x_1} = \frac{y_1''' U_{11} - x_1''' U_{21}}{(x_1''')^2 + (y_1''')^2} \tag{A.35}$$

with $\frac{\partial B_1'''}{\partial y_1}$ and $\frac{\partial B_1'''}{\partial z_1}$ following similarly.

Bearing in Remote Stabilized Coordinates

In this instance

$$\tan B_2 = \frac{x_2}{y_2} \tag{A.36}$$

where x_2 and y_2 are found from (A.18) and (A.25) as

$$x_2 = \begin{bmatrix} 1 & 0 & 0 \end{bmatrix} N \begin{bmatrix} x_1 + \Delta R_{x1} \\ y_1 + \Delta R_{y1} \\ z_1 + \Delta R_{z1} \end{bmatrix} \tag{A.37}$$

$$= N_{11}(x_1 + \Delta R_{x1}) + N_{12}(y_1 + \Delta R_{y2}) + N_{13}(z_1 + \Delta R_{z1}) \tag{A.38}$$

$$y_2 = \begin{bmatrix} 0 & 1 & 0 \end{bmatrix} N \begin{bmatrix} x_1 + \Delta R_{x1} \\ y_1 + \Delta R_{y1} \\ z_1 + \Delta R_{z1} \end{bmatrix} \tag{A.39}$$

$$= N_{21}(x_1 + \Delta R_{x1}) + N_{22}(y_1 + \Delta R_{y2}) + N_{23}(z_1 + \Delta R_{z1}) \tag{A.40}$$

Derivatives also follow from (A.27) with $u = x_2$ and $v = y_2$ so that

$$\frac{\partial B_2}{\partial x_1} = \frac{y_2 N_{11} - x_2 N_{21}}{x_2^2 + y_2^2} \tag{A.41}$$

with $\frac{\partial B_2}{\partial y_1}$ and $\frac{\partial B_2}{\partial z_1}$ following similarly.

Bearing in Remote Deck Coordinates

For this final instance, where

$$\tan B_2''' = \frac{x_2'''}{y_2'''} \tag{A.42}$$

(A.26) dictates that

$$x_2''' = V_{11}(x_1 + \Delta R_{x1}) + V_{12}(y_1 + \Delta R_{y2}) + V_{13}(z_1 + \Delta R_{z1}) \tag{A.43}$$
$$y_2''' = V_{21}(x_1 + \Delta R_{x1}) + V_{22}(y_1 + \Delta R_{y2}) + V_{23}(z_1 + \Delta R_{z1}) \tag{A.44}$$

Thus, the derivatives take the form

$$\frac{\partial B_2'''}{\partial x_1} = \frac{y_2''' V_{11} + x_2''' V_{21}}{(x_2''')^2 + (y_2''')^2} \tag{A.45}$$

with $\frac{\partial B_2'''}{\partial y_1}$ and $\frac{\partial B_2'''}{\partial z_1}$ following similarly.

Tables of M_p and H

Tables A–1 through A–4 formulas cover the four coordinate systems that have been introduced. It is assumed that when a remote coordinate system is used that

$$\Delta R_1 = \begin{bmatrix} \Delta R_{x1} & \Delta R_{y1} & \Delta R_{z1} \end{bmatrix}^T \tag{A.46}$$

and coordinate rotation matrix N have been precomputed. Also, when a deck coordinate system is used, precomputation of the appropriate coordinate rotation matrices $R^{(i)}$, $P^{(i)}$, and $H^{(i)}$ is assumed.

The user should also note that these formulations involve coordinate transformations of $\begin{bmatrix} \cdots & \dot{x} & \cdots & \dot{y} & \cdots & \dot{z} \end{bmatrix}^T$ that do not use platform velocity as input. This means that it is implicitly assumed that the target velocity is much larger than that of the ship. While usually true, this assumption may noticeably degrade the otherwise high accuracy of doppler radar measurements.

Table A-1. Formulas for Local Stabilized Coordinates

(A) Bearing

$$M_p = B_1 \triangleq \tan^{-1}\frac{x_1}{y_1} \qquad H = \left[\begin{array}{cccccc} \frac{\partial B_1}{\partial x_1} & 0 & \frac{\partial B_1}{\partial y_1} & 0 & 0 & 0 \end{array}\right]$$

$$\frac{\partial B_1}{\partial x_1} = \frac{y_1}{x_1^2 + y_1^2} \qquad \frac{\partial B_1}{\partial y_1} = \frac{-x_1}{x_1^2 + y_1^2}$$

(B) Slant range

$$M_p = s_1 = \sqrt{x_1^2 + y_1^2 + z_1^2} \qquad H = \left[\begin{array}{cccccc} \frac{\partial s_1}{\partial x_1} & 0 & \frac{\partial s_1}{\partial y_1} & 0 & \frac{\partial s_1}{\partial z_1} & 0 \end{array}\right]$$

$$\frac{\partial s_1}{\partial x_1} = \frac{x_1}{s_1} \qquad \frac{\partial s_1}{\partial y_1} = \frac{y_1}{s_1}$$

$$\frac{\partial s_1}{\partial z_1} = \frac{z_1}{s_1}$$

(C) Elevation

$$M_p = E_1 = \tan^{-1}\frac{z_1}{\sqrt{x_1^2 + y_1^2}} \qquad H = \left[\begin{array}{cccccc} \frac{\partial E_1}{\partial x_1} & 0 & \frac{\partial E_1}{\partial y_1} & 0 & \frac{\partial E_1}{\partial z_1} & 0 \end{array}\right]$$

$$\frac{\partial E_1}{\partial x_1} = \left(\frac{-1}{s_1^2}\right)\frac{x_1 z_1}{\sqrt{x_1^2 + y_1^2}} \qquad \frac{\partial E_1}{\partial y_1} = \left(\frac{-1}{s_1^2}\right)\frac{y_1 z_1}{\sqrt{x_1^2 + y_1^2}}$$

$$\frac{\partial E_1}{\partial z_1} = \left(\frac{1}{s_1^2}\right)\sqrt{x_1^2 + y_1^2}$$

(D) Doppler

$$M_p = \dot{s}_1 = \frac{d}{dt}\sqrt{x_1^2 + y_1^2 + z_1^2} \qquad H = \left[\begin{array}{cccccc} \frac{\partial \dot{s}_1}{\partial x_1} & \frac{\partial \dot{s}_1}{\partial \dot{x}_1} & \frac{\partial \dot{s}_1}{\partial y_1} & \frac{\partial \dot{s}_1}{\partial \dot{y}_1} & \frac{\partial \dot{s}_1}{\partial z_1} & \frac{\partial \dot{s}_1}{\partial \dot{z}_1} \end{array}\right]$$

$$\frac{\partial \dot{s}_1}{\partial x_1} = \frac{\dot{x}_1}{s_1} - \frac{x_1(x_1\dot{x}_1 + y_1\dot{y}_1 + z_1\dot{z}_1)}{s_1^3} \qquad \frac{\partial \dot{s}_1}{\partial \dot{x}_1} = \frac{x_1}{s_1}$$

$$\frac{\partial \dot{s}_1}{\partial y_1} = \frac{\dot{y}_1}{s_1} - \frac{y_1(x_1\dot{x}_1 + y_1\dot{y}_1 + z_1\dot{z}_1)}{s_1^3} \qquad \frac{\partial \dot{s}_1}{\partial \dot{y}_1} = \frac{y_1}{s_1}$$

$$\frac{\partial \dot{s}_1}{\partial z_1} = \frac{\dot{z}_1}{s_1} - \frac{z_1(x_1\dot{x}_1 + y_1\dot{y}_1 + z_1\dot{z}_1)}{s_1^3} \qquad \frac{\partial \dot{s}_1}{\partial \dot{z}_1} = \frac{z_1}{s_1}$$

Table A-2. Formulas for Local Deck Coordinates

(A) Bearing

$$M_p = B_1''' \stackrel{=}{\tan}^{-1} \frac{x_1'''}{y_1'''} \qquad H = \left[\frac{\partial B_1'''}{\partial x_1} \quad 0 \quad \frac{\partial B_1'''}{\partial y_1} \quad 0 \quad \frac{\partial B_1'''}{\partial z_1} \quad 0 \right]$$

$$x_1''' = x_1 U_{11} + y_1 U_{12} + z_1 U_{13} \qquad y_1''' = x_1 U_{21} + y_1 U_{22} + z_1 U_{23} \qquad z_1''' = x_1 U_{31} + y_1 U_{32} + z_1 U_{33}$$

$$\frac{\partial B_1'''}{\partial x_1} = \frac{y_1''' U_{11} - x_1''' U_{21}}{(x_1''')^2 + (y_1''')^2} \qquad \frac{\partial B_1'''}{\partial y_1} = \frac{y_1''' U_{12} - x_1''' U_{22}}{(x_1''')^2 + (y_1''')^2} \qquad \frac{\partial B_1'''}{\partial z_1} = \frac{y_1''' U_{13} - x_1''' U_{23}}{(x_1''')^2 + (y_1''')^2}$$

(B) Slant range

$$M_p = s_1''' = s_1 = \sqrt{x_1^2 + y_1^2 + z_1^2} \qquad H = \left[\frac{\partial s_1'''}{\partial x_1} \quad 0 \quad \frac{\partial s_1'''}{\partial y_1} \quad 0 \quad \frac{\partial s_1'''}{\partial z_1} \quad 0 \right]$$

$$\frac{\partial s_1'''}{\partial x_1} = \frac{x_1''' U_{11} + y_1''' U_{12} + z_1''' U_{13}}{s_1} \qquad \frac{\partial s_1'''}{\partial y_1} = \frac{x_1''' U_{21} + y_1''' U_{22} + z_1''' U_{23}}{s_1} \qquad \frac{\partial s_1'''}{\partial z_1} = \frac{x_1''' U_{31} + y_1''' U_{32} + z_1''' U_{33}}{s_1}$$

(C) Elevation

$$M_p = E_1''' = \tan^{-1} \frac{z_1'''}{\sqrt{(x_1''')^2 + (y_1''')^2}} \qquad H = \left[\frac{\partial E_1'''}{\partial x_1} \quad 0 \quad \frac{\partial E_1'''}{\partial y_1} \quad 0 \quad \frac{\partial E_1'''}{\partial z_1} \quad 0 \right]$$

$$\alpha = (x_1''')^2 + (y_1''')^2 + (z_1''')^2$$

$$\gamma = \sqrt{(x_1''')^2 + (y_1''')^2}$$

$$\frac{\partial E_1'''}{\partial x_1} = \frac{1}{\alpha}\left[\gamma U_{31} - \frac{z_1'''}{\gamma}(x_1''' U_{11} + y_1''' U_{21})\right]$$

$$\frac{\partial E_1'''}{\partial y_1} = \frac{1}{\alpha}\left[\gamma U_{32} - \frac{z_1'''}{\gamma}(x_1''' U_{12} + y_1''' U_{22})\right]$$

$$\frac{\partial E_1'''}{\partial z_1} = \frac{1}{\alpha}\left[\gamma U_{33} - \frac{z_1'''}{\gamma}(x_1''' U_{13} + y_1''' U_{23})\right]$$

(D) Doppler

$$M_p = \dot{s}_1''' = \frac{d}{dt}\sqrt{(x_1''')^2 + (y_1''')^2 + (z_1''')^2} \qquad H = \left[\frac{\partial \dot{s}_1'''}{\partial x_1} \quad \frac{\partial \dot{s}_1'''}{\partial \dot{x}_1} \quad \frac{\partial \dot{s}_1'''}{\partial y_1} \quad \frac{\partial \dot{s}_1'''}{\partial \dot{y}_1} \quad \frac{\partial \dot{s}_1'''}{\partial z_1} \quad \frac{\partial \dot{s}_1'''}{\partial \dot{z}_1} \right]$$

$$\dot{x}_1''' = \dot{x}_1 U_{11} + \dot{y}_1 U_{12} + \dot{z}_1 U_{13} \qquad \dot{y}_1''' = \dot{x}_1 U_{21} + \dot{y}_1 U_{22} + \dot{z}_1 U_{23} \qquad \dot{z}_1''' = \dot{x}_1 U_{31} + \dot{y}_1 U_{32} + \dot{z}_1 U_{33}$$

$$\eta = x_1''' \dot{x}_1''' + y_1''' \dot{y}_1''' + z_1''' \dot{z}_1'''$$

$$\frac{\partial \dot{s}_1'''}{\partial x_1} = \frac{\dot{x}_1}{s_1} - \frac{\eta x_1}{s_1^3} \qquad \frac{\partial \dot{s}_1'''}{\partial y_1} = \frac{\dot{y}_1}{s_1} - \frac{\eta y_1}{s_1^3} \qquad \frac{\partial \dot{s}_1'''}{\partial z_1} = \frac{\dot{z}_1}{s_1} - y\frac{\eta z_1}{s_1^3}$$

$$\frac{\partial \dot{s}_1'''}{\partial \dot{x}_1} = \frac{x_1}{s_1} \qquad \frac{\partial \dot{s}_1'''}{\partial \dot{y}_1} = \frac{y_1}{s_1} \qquad \frac{\partial \dot{s}_1'''}{\partial \dot{z}_1} = \frac{z_1}{s_1}$$

Table A-3. Formulas for Remote Stabilized Coordinates

(A) Bearing

$$M_p = B_2 \overset{\pi}{\tan}^{-1} \frac{x_2}{y_2} \qquad H = \begin{bmatrix} \frac{\partial B_2}{\partial x_1} & 0 & \frac{\partial B_2}{\partial y_1} & 0 & \frac{\partial B_2}{\partial z_1} & 0 \end{bmatrix}$$

$$x_2 = N_{11}(x_1 + \Delta R_{x1}) + N_{12}(y_1 + \Delta R_{y1}) + N_{13}(z_1 + \Delta R_{z1})$$
$$y_2 = N_{21}(x_1 + \Delta R_{x1}) + N_{22}(y_1 + \Delta R_{y1}) + N_{23}(z_1 + \Delta R_{z1})$$
$$z_2 = N_{31}(x_1 + \Delta R_{x1}) + N_{32}(y_1 + \Delta R_{y1}) + N_{33}(z_1 + \Delta R_{z1})$$

$$\frac{\partial B_2}{\partial x_1} = \frac{y_2 N_{11} - x_1 N_{21}}{x_2^2 + y_2^2} \qquad \frac{\partial B_2}{\partial y_1} = \frac{y_1 N_{12} - x_2 N_{22}}{x_2^2 + y_2^2} \qquad \frac{\partial B_2}{\partial z_1} = \frac{y_1 N_{13} - x_2 N_{23}}{x_2^2 + y_2^2}$$

(B) Slant range

$$M_p = s_2 = \sqrt{x_2^2 + y_2^2 + z_2^2} \qquad H = \begin{bmatrix} \frac{\partial s_2}{\partial x_1} & 0 & \frac{\partial s_2}{\partial y_1} & 0 & \frac{\partial s_2}{\partial z_1} & 0 \end{bmatrix}$$

$$\frac{\partial s_2}{\partial x_1} = \frac{x_1 + \Delta R_{x1}}{s_2} \qquad \frac{\partial s_2}{\partial y_1} = \frac{y_1 + \Delta R_{y1}}{s_2} \qquad \frac{\partial s_2}{\partial z_2} = \frac{z_1 + \Delta R_{z1}}{s_2}$$

(C) Elevation

$$M_p = E_2 = \tan^{-1} \frac{z_2}{\sqrt{x_2^2 + y_2^2}} \qquad H = \begin{bmatrix} \frac{\partial E_2}{\partial x_1} & 0 & \frac{\partial E_2}{\partial y_1} & 0 & \frac{\partial E_2}{\partial z_1} & 0 \end{bmatrix}$$

$$\alpha = x_2^2 + y_2^2 + z_2^2 \qquad \frac{\partial E_2}{\partial x_1} = \frac{1}{\alpha}\left[\gamma N_{31} - \frac{z_2}{\gamma}(x_2 N_{11} + y_2 N_{21})\right]$$

$$\gamma = \sqrt{x_2^2 + y_2^2} \qquad \frac{\partial E_2}{\partial y_1} = \frac{1}{\alpha}\left[\gamma N_{32} - \frac{z_2}{\gamma}(x_2 N_{12} + y_2 N_{22})\right]$$

$$\frac{\partial E_2}{\partial z_1} = \frac{1}{\alpha}\left[\gamma N_{33} - \frac{z_2}{\gamma}(x_2 N_{13} + y_2 N_{23})\right]$$

(D) Doppler

$$M_p = \dot{s}_2 = \frac{d}{dt}\sqrt{x_2^2 + y_2^2 + z_2^2} \qquad H = \begin{bmatrix} \frac{\partial \dot{s}_2}{\partial x_1} & \frac{\partial \dot{s}_2}{\partial \dot{x}_1} & \frac{\partial \dot{s}_2}{\partial y_1} & \frac{\partial \dot{s}_2}{\partial \dot{y}_1} & \frac{\partial \dot{s}_2}{\partial z_1} & \frac{\partial \dot{s}_2}{\partial \dot{z}_1} \end{bmatrix}$$

$$\dot{x}_2 = \dot{x}_1 N_{11} + \dot{y}_1 N_{12} + \dot{z}_1 N_{13} \qquad \dot{y}_2 = \dot{x}_1 N_{21} + \dot{y}_1 N_{22} + \dot{z}_1 N_{23} \qquad \dot{z}_2 = \dot{x}_1 N_{31} + \dot{Y}_1 N_{32} + \dot{z}_1 N_{33}$$

$$\eta = x_2 \dot{x}_2 + y_2 \dot{y}_2 + z_2 \dot{z}_2$$

$$\frac{\partial \dot{s}_2}{\partial x_1} = \frac{\dot{x}_1}{s_2} - \frac{\eta(x_1 + \Delta R_{x1})}{s_2^3} \qquad \frac{\partial \dot{s}_2}{\partial y_1} = \frac{\dot{y}_1}{s_2} - \frac{\eta(y_1 + \Delta R_{y1})}{s_2^3} \qquad \frac{\partial \dot{s}_2}{\partial z_1} = \frac{\dot{z}_1}{s_2} - \frac{\eta(z_1 + \Delta R_{z1})}{s_2^3}$$

$$\frac{\partial \dot{s}_2}{\partial \dot{x}_1} = \frac{x_1 + \Delta R_{x1}}{s_2} \qquad \frac{\partial \dot{s}_2}{\partial \dot{y}_1} = \frac{y_1 + \Delta R_{y1}}{s_2} \qquad \frac{\partial \dot{s}_2}{\partial \dot{z}_1} = \frac{z_1 + \Delta R_{z1}}{s_2}$$

Table A–4. Formulas for Remote Deck Coordinates

(A) Bearing

$$M_p = B_2''' \stackrel{=}{\tan}^{-1} \frac{x_2'''}{y_2'''} \qquad H = \left[\frac{\partial B_2'''}{\partial x_1} \quad 0 \quad \frac{\partial B_2'''}{\partial y_1} \quad 0 \quad \frac{\partial B_2'''}{\partial z_1} \quad 0 \right]$$

$$\begin{aligned} x_2''' &= V_{11}(x_1 + \Delta R_{x1}) + V_{12}(y_1 + \Delta R_{y1}) + V_{13}(z_1 + \Delta R_{z1}) \\ y_2''' &= V_{21}(x_1 + \Delta R_{x1}) + V_{22}(y_1 + \Delta R_{y1}) + V_{23}(z_1 + \Delta R_{z1}) \\ z_2''' &= V_{31}(x_1 + \Delta R_{x1}) + V_{32}(y_1 + \Delta R_{y1}) + V_{33}(z_1 + \Delta R_{z1}) \end{aligned}$$

$$\frac{\partial B_2'''}{\partial x_1} = \frac{y_2'''V_{11} - x_2'''V_{21}}{(x_2''')^2 + (y_2''')^2} \qquad \frac{\partial B_2'''}{\partial y_1} = \frac{y_2'''V_{12} - x_2'''V_{22}}{(x_2''')^2 + (y_2''')^2} \qquad \frac{\partial B_2'''}{\partial z_1} = \frac{y_2'''V_{13} - x_2'''V_{23}}{(x_2''')^2 + (y_2''')^2}$$

(B) Slant range

$$M_p = s_2''' = \sqrt{(x_2''')^2 + (y_2''')^2 + (z_2''')^2} \qquad H = \left[\frac{\partial s_2'''}{\partial x_1} \quad 0 \quad \frac{\partial s_2'''}{\partial y_1} \quad 0 \quad \frac{\partial s_2'''}{\partial z_1} \quad 0 \right]$$

$$\frac{\partial s_2'''}{\partial x_1} = \frac{x_1 + \Delta R_{x1}}{s_2'''} \qquad \frac{\partial s_2'''}{\partial y_1} = \frac{y_1 + \Delta R_{y1}}{s_2'''} \qquad \frac{\partial s_2'''}{\partial z_2} = \frac{z_1 + \Delta R_{z1}}{s_2'''}$$

(C) Elevation

$$M_p = E_2''' = \tan^{-1} \frac{z_2'''}{\sqrt{(x_2''')^2 + (y_2''')^2}} \qquad H = \left[\frac{\partial E_2'''}{\partial x_1} \quad 0 \quad \frac{\partial E_2'''}{\partial y_1} \quad 0 \quad \frac{\partial E_2'''}{\partial z_1} \quad 0 \right]$$

$$\alpha = (x_2''')^2 + (y_2''')^2 + (z_2''')^2$$

$$\gamma = \sqrt{(x_2''')^2 + (y_2''')^2}$$

$$\frac{\partial E_2'''}{\partial x_1} = \frac{1}{\alpha}\left[\gamma V_{31} - \frac{z_2'''}{\gamma}(x_2'''V_{11} + y_2'''V_{21})\right]$$

$$\frac{\partial E_2'''}{\partial y_1} = \frac{1}{\alpha}\left[\gamma V_{32} - \frac{z_2'''}{\gamma}(x_2'''V_{12} + y_2'''V_{22})\right]$$

$$\frac{\partial E_2'''}{\partial z_1} = \frac{1}{\alpha}\left[\gamma V_{33} - \frac{z_2'''}{\gamma}(x_2'''V_{13} + y_2'''V_{23})\right]$$

(D) Doppler

$$M_p = \dot{s}_2''' = \frac{d}{dt}\sqrt{(x_2''')^2 + (y_2''')^2 + (z_2''')^2} \qquad H = \left[\frac{\partial \dot{s}_2'''}{\partial x_1} \quad \frac{\partial \dot{s}_2'''}{\partial \dot{x}_1} \quad \frac{\partial \dot{s}_2'''}{\partial y_1} \quad \frac{\partial \dot{s}_2'''}{\partial \dot{y}_1} \quad \frac{\partial \dot{s}_2'''}{\partial z_1} \quad \frac{\partial \dot{s}_2'''}{\partial \dot{z}_1} \right]$$

$$\dot{x}_2''' = \dot{x}_1'''V_{11} + \dot{y}_1'''V_{12} + \dot{z}_1'''V_{13} \qquad \dot{y}_2''' = \dot{x}_1'''V_{21} + \dot{y}_1'''V_{22} + \dot{z}_1'''V_{23} \qquad \dot{z}_2''' = \dot{x}_1'''V_{31} + \dot{Y}_1'''V_{32} + \dot{z}_1'''V_{33}$$

$$\eta = x_2'''\dot{x}_2''' + y_2'''\dot{y}_2''' + z_2'''\dot{z}_2'''$$

$$\frac{\partial \dot{s}_2'''}{\partial x_1} = \frac{\dot{x}_1}{s_2'''} - \frac{\eta(x_1 + \Delta R_{x1})}{(s_2''')^3} \qquad \frac{\partial \dot{s}_2'''}{\partial y_1} = \frac{\dot{y}_1}{s_2'''} - \frac{\eta(y_1 + \Delta R_{y1})}{(s_2''')^3} \qquad \frac{\partial \dot{s}_2'''}{\partial z_1} = \frac{\dot{z}_1}{s_2'''} - \frac{\eta(z_1 + \Delta R_{z1})}{(s_2''')^3}$$

$$\frac{\partial \dot{s}_2'''}{\partial \dot{x}_1} = \frac{x_1 + \Delta R_{x1}}{s_2'''} \qquad \frac{\partial \dot{s}_2'''}{\partial \dot{y}_1} = \frac{y_1 + \Delta R_{y1}}{s_2'''} \qquad \frac{\partial \dot{s}_2'''}{\partial \dot{z}_1} = \frac{z_1 + \Delta R_{z1}}{s_2'''}$$

DISTRIBUTION

	Copies
DOD ACTIVITIES (CONUS):	
ATTN DR RABINDER MADAN CODE 1114SE CHIEF OF NAVAL RESEARCH 800 N QUINCY ST ARLINGTON VA 22217-5000	1
ATTN LTCD CHAMPION 400B30C2 NAVAL SEA SYSTEMS COMMAND 2531 JEFFERSON DAVIS HWY ARLINGTON VA 22242-5160	1
ATTN CAPT BINGAY PEOTAD-D22 NAVAL SEA SYSTEMS COMMAND 2531 JEFFERSON DAVIS HWY ARLINGTON VA 22242-5160	1
ATTN IRVIN OLIN CODE 5301 NAVAL RESEARCH LABORATORY 4555 OVERLOOK DR SW WASHIGTON DC 20371-5320	1
ATTN PAUL HUGHES CODE 5312 NAVAL RESEARCH LABORATORY 4555 OVERLOOK DR SW WASHIGTON DC 20371-5320	1
ATTN JERRY TRUNK CODE 5310 NAVAL RESEARCH LABORATORY 4555 OVERLOOK DR SW WASHIGTON DC 20375-5320	1

	Copies
DOD ACTIVITIES (CONUS)(CONTINUED):	
ATTN GEORGE SIOURIS ASC/ENSSC WRIGHT PATTERSON AFB OH 45433	1
DEFENSE TECHNICAL INFORMATION CENTER CAMERON STATION ALEXANDRIA VA 22304-6145	12
NON-DOD ACTIVITIES:	
ATTN DR GLENN M SPARKS ANTHONY VIDMAR JR GOVERNMENT ELECTRONIC SYSTEMS DIVISION MOORESTOWN NJ 08057	1 1
ATTN PROF YAAKOV BAR SALOAM ESE DEPARTMENT U157 260 GLENBROOK RD STORRS CT 06269-3157	1
ATTN OLIVER E DRUMMOND HUGHES MISSILE SYSTEM CO 10900 E 4TH ST MZ 601 75 RANCHO CUCAMONGA CA 91730	1
ATTN GIFT AND EXCHANGE DIV LIBRARY OF CONGRESS WASHINGTON DC 20540	4

DISTRIBUTION (CONTINUED)

NON-DOD ACTIVITIES (CONTINUED):	Copies
ATTN DR J N ANDERSON	1
A T ALOUANI	1
P K RAJAN	1
DEPT OF ELECTRICAL ENGIN	
TENNESSEE TECH UNIVERSITY	
TTU BOX 05005	
COOKEVILLE TN 38505	
ATTN DR PAUL KALATA	1
ECE DEPARTMENT	
DREXEL UNIVERSITY	
PHILADELPHIA PA 19104	
ATTN SAMUEL S. BLACKMAN	1
HUGHES AIRCRAFT	
EO/E1	
MAILSTOP B102	
PO BOX 902	
ELSUGUNGO CA 90245	
ATTN EDWARD PRICE	1
LON CARPENTER	1
FMC CORPORATION	
1 DANUBE DR	
KING GEORGE VA 22485	
ATTN JOSEPH S PRIMERANO	1
RAYTHEON	
PO BOX 161	
DAHLGREN VA 22448	
ATTN GLENN WOODARD	1
SYSCON CORPORATION	
TIDEWATER DIVISION	
PO BOX 1480	
DAHLGREN VA 22448-1480	

NON-DOD ACTIVITIES (CONTINUED):	Copies
ATTN F R CASTELLA	5
APPLIED PHYSICS LABORATORY	
THE JOHNS HOPKINS UNIVERSITY	
11000 JOHNS HOPKINS RD	
LAUREL MD 20723-6099	

INTERNAL DISTRIBUTION :		Copies
A20	(BEUGLASS)	1
A20	(LUCAS)	1
B		1
B05	(STATON)	1
B30		1
B32	(BLAIR)	20
B32	(CONTE)	1
B32	(GENTRY)	1
B32	(GRAY)	1
B32	(HELMICK)	1
B32	(HILTON)	20
B32	(MARTIN)	5
B32	(RICE)	1
B32	(WATSON)	1
B35	(BAILEY)	1
B35	(FENNEMORE)	1
E231		3
E281	(LIPSCOMB)	1
F		1
F07		1
F07	(AUGER)	1
F11	(DOSSETT)	1
F21		1
F21	(PARKER)	1
F30		1
F307	(WILSON)	1

DISTRIBUTION (CONTINUED)

Copies

INTERNAL DISTRIBUTION (CONTINUED):

F32	(BOYKIN)	1
F33		1
F33	(AFRICA)	1
F406		1
F41	(KNICELEY)	1
F41	(MARTIN)	1
F42	(KLOCHAK)	1
F43	(FONTANA)	2
F44		1
G		1
G23	(BIBEL, JOHN)	1
G23	(GRAFF)	1
N05		1
N05	(GASTON)	1
N07		1
N24		1
N24	(BAILEY)	1
N24	(BOYER)	1
N24	(BURROW)	1
N24	(HANSEN)	1
N24	(MILLER)	1
N24	(SERAKOS)	1
N74	(GIDEP)	1
N84	(HART)	1
N84	(LAMBERTSON)	1
N84	(MCNATT)	1
N84	(MURRAY)	1
N84	(PALEN)	1

REPORT DOCUMENTATION PAGE

Form Approved
OMB No. 0704-0188

1. AGENCY USE ONLY *(Leave blank)*	2. REPORT DATE	3. REPORT TYPE AND DATES COVERED
	August 1993	Final

4. TITLE AND SUBTITLE
Tracking with Time-Delayed Data in Multisensor Systems

5. FUNDING NUMBERS

6. AUTHOR(S)
Richard D. Hilton, David A. Martin, William D. Blair

7. PERFORMING ORGANIZATION NAME(S) AND ADDRESS(ES)
Naval Surface Warfare Center
Dahlgren Division (Code B32)
Dahlgren, Virginia 22448-5000

8. PERFORMING ORGANIZATION REPORT NUMBER
NSWCDD/TR-93/351

9. SPONSORING/MONITORING AGENCY NAME(S) AND
AEGIS Program Office
Code N05
Dahlgren, Virginia 22448-5000

10. SPONSORING/MONITORING AGENCY REPORT NUMBER

11. SUPPLEMENTARY NOTES

12a. DISTRIBUTION/AVAILABILITY
Approved for public release; distribution is unlimited.

12b. DISTRIBUTION CODE

13. ABSTRACT *(Maximum 200 words)*

When techniques for target tracking are expanded to make use of multiple sensors in a multiplatform system, the possibility of time delayed data becomes a reality. When a discrete-time Kalman filter is applied and some of the data entering the filter are delayed, proper processing of these late data is a necessity for obtaining an "optimal" estimate of a target's state. If this problem is not given special care, the quality of the state estimates can be degraded relative to that quality provided by a single sensor. A negative-time update technique is developed using the criteria of minimum mean-square error (MMSE) under the constraint that only the results of the most recent update are saved. The performance of the MMSE technique is compared to that of the ad hoc approach employed in the Cooperative Engagement Capabilities (CEC) system for processing data from multiple platforms. It was discovered that the MMSE technique is a stable solution to the negative-time update problem, while the CEC technique was found to be less than desirable when used with filters designed for tracking highly maneuvering targets at relatively low data rates. The MMSE negative-time update technique was found to be a superior alternative to the existing CEC negative-time update technique.

14. SUBJECT TERMS	15. NUMBER OF PAGES
Multisensor Systems, Kalman Filter, Cooperative Engagement Capabilities (CEC) Technique, Minimum Mean-sQuare Error (MMSE) Technique	57
	16. PRICE CODE

17. SECURITY CLASSIFICATION OF REPORT	18. SECURITY CLASSIFICATION OF THIS PAGE	19. SECURITY CLASSIFICATION OF ABSTRACT	20. LIMITATION OF ABSTRACT
UNCLASSIFIED	UNCLASSIFIED	UNCLASSIFIED	SAR

GENERAL INSTRUCTIONS FOR COMPLETING SF 298

The Report Documentation Page (RDP) is used in announcing and cataloging reports. It is important that this information be consistent with the rest of the report, particularly the cover and its title page. Instructions for filling in each block of the form follow. It is important to ***stay within the lines*** to meet ***optical scanning requirements***.

Block 1. Agency Use Only *(Leave blank)*.

Block 2. Report Date. Full publication date including day, month, and year, if available (e.g. 1 Jan 88). Must cite at least the year.

Block 3. Type of Report and Dates Covered. State whether report is interim, final, etc. If applicable, enter inclusive report dates (e.g. 10 Jun 87 - 30 Jun 88).

Block 4. Title and Subtitle. A title is taken from the part of the report that provides the most meaningful and complete information. When a report is prepared in more than one volume, repeat the primary title, add volume number, and include subtitle for the specific volume. On classified documents enter the title classification in parentheses.

Block 5. Funding Numbers. To include contract and grant numbers; may include program element number(s), project number(s), task number(s), and work unit number(s). Use the following labels:

C	- Contract	**PR**	- Project
G	- Grant	**TA**	- Task
PE	- Program Element	**WU**	- Work Unit Accession No.

BLOCK 6. Author(s). Name(s) of person(s) responsible for writing the report, performing the research, or credited with the content of the report. If editor or compiler, this should follow the name(s).

Block 7. Performing Organization Name(s) and address(es). Self-explanatory.

Block 8. Performing Organization Report Number. Enter the unique alphanumeric report number(s) assigned by the organization performing the report.

Block 9. Sponsoring/Monitoring Agency Name(s) and Address(es). Self-explanatory.

Block 10. Sponsoring/Monitoring Agency Report Number. *(If Known)*

Block 11. Supplementary Notes. Enter information not included elsewhere such as: Prepared in cooperation with...; Trans. of...; To be published in... . When a report is revised, include a statement whether the new report supersedes or supplements the older report.

Block 12a. Distribution/Availability Statement. Denotes public availability or limitations. Cite any availability to the public. Enter additional limitations or special markings in all capitals (e.g. NOFORN, REL, ITAR).

DOD	-	See DoDD 5230.24, "Distribution Statements on Technical Documents."
DOE	-	See authorities.
NASA	-	See Handbook NHB 2200.2
NTIS	-	Leave blank

Block 12b. Distribution Code.

DOD	-	Leave blank.
DOE	-	Enter DOE distribution categories from the Standard Distribution for Unclassified Scientific and Technical Reports.
NASA	-	Leave blank.
NTIS	-	Leave blank.

Block 13. Abstract. Include a brief ***(Maximum 200 words)*** factual summary of the most significant information contained in the report.

Block 14. Subject Terms. Keywords or phrases identifying major subjects in the report.

Block 15. Number of Pages. Enter the total number of pages.

Block 16. Price Code. Enter appropriate price code ***(NTIS only)***

Block 17.-19. Security Classifications. Self-explanatory. Enter U.S. Security Classification in accordance with U.S. Security Regulations (i.e., UNCLASSIFIED). If form contains classified information, stamp classification on the top and bottom of this page.

Block 20. Limitation of Abstract. This block must be completed to assign a limitation to the abstract. Enter either UL (unlimited or SAR (same as report). An entry in this block is necessary if the abstract is to be limited. If blank, the abstract is assumed to be unlimited.